Recent ALICE experimental results on ultra-peripheral collisions

Adam Matyja

Institute of Nuclear Physics
Polish Academy of Sciences, Kraków

Białasówka seminar
Kraków

19 May 2023, Kraków

Outline

- Introduction
- Experimental apparatus
- Mesurements
  - Coherent and incoherent J/ψ photoproduction in Pb-Pb
  - Coherent $\psi(2S)$ photoproduction in Pb-Pb
  - Exclusive and dissociative J/ψ photoproduction in p-Pb
  - Neutron emission
  - Coherent ρ^0 photoproduction in Pb-Pb and Xe-Xe
  - Excited ρ state photoproduction
- Future plans
- Summary

Ultra-peripheral collisions (UPC)

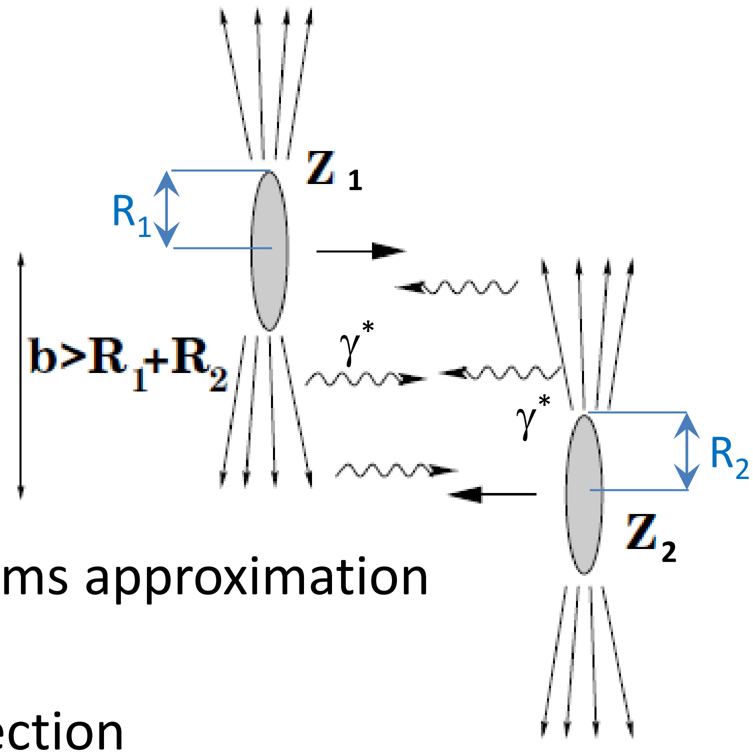

- Impact parameter $b > R_1 + R_2$
  - Hadronic interactions suppressed
- Photon induced reactions:
  - Well described in Weizsäcker-Williams approximation
  - Photon flux ~ Z^2 (Z_{Pb} = 82)
  - Large γ-induced interaction cross section
- Clear signature:
  - Low detector activity
  - Rapidity gap(s)

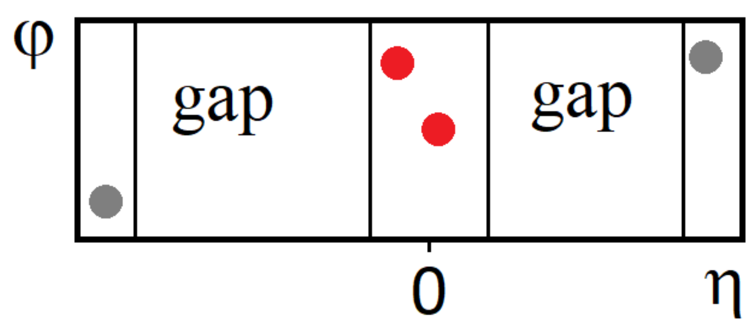

Photoproduction and main variables

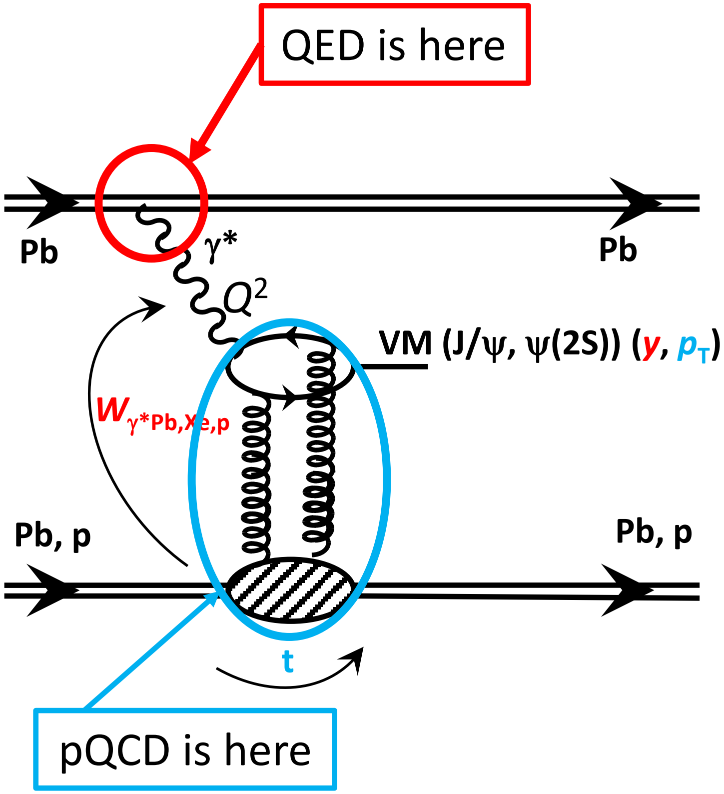

- Hard scale assured by high mass states i.e. J/ψ ,$\psi(2S)$
- Semi-hard scale for ρ^0

- Photon $Q^2 \sim M_{VM}{}^2 / 4$
- Vector Meson (VM) quantum numbers:
  - $J^{PC} = 1^{--}$
- Bjorken-*x:* fraction of longitudinal momentum of proton

$$x_B = \frac{M_{VM}}{\sqrt{s_{NN}}} e^{\pm y}$$

  - Photoproduction is sensitive to gluon density evolution at low x_B at LO
  - There are new NLO calculations
- Photon-target center-of-mass energy

$$W^2_{\gamma^* Pb,p} = 2E_{Pb,p} M_{VM} e^{\mp y}$$

- 4-momentum transfer t
  - Gluon distribution in the transverse plane $|t| \sim p_T{}^2$

J/ψ photoproduction – LO vs NLO

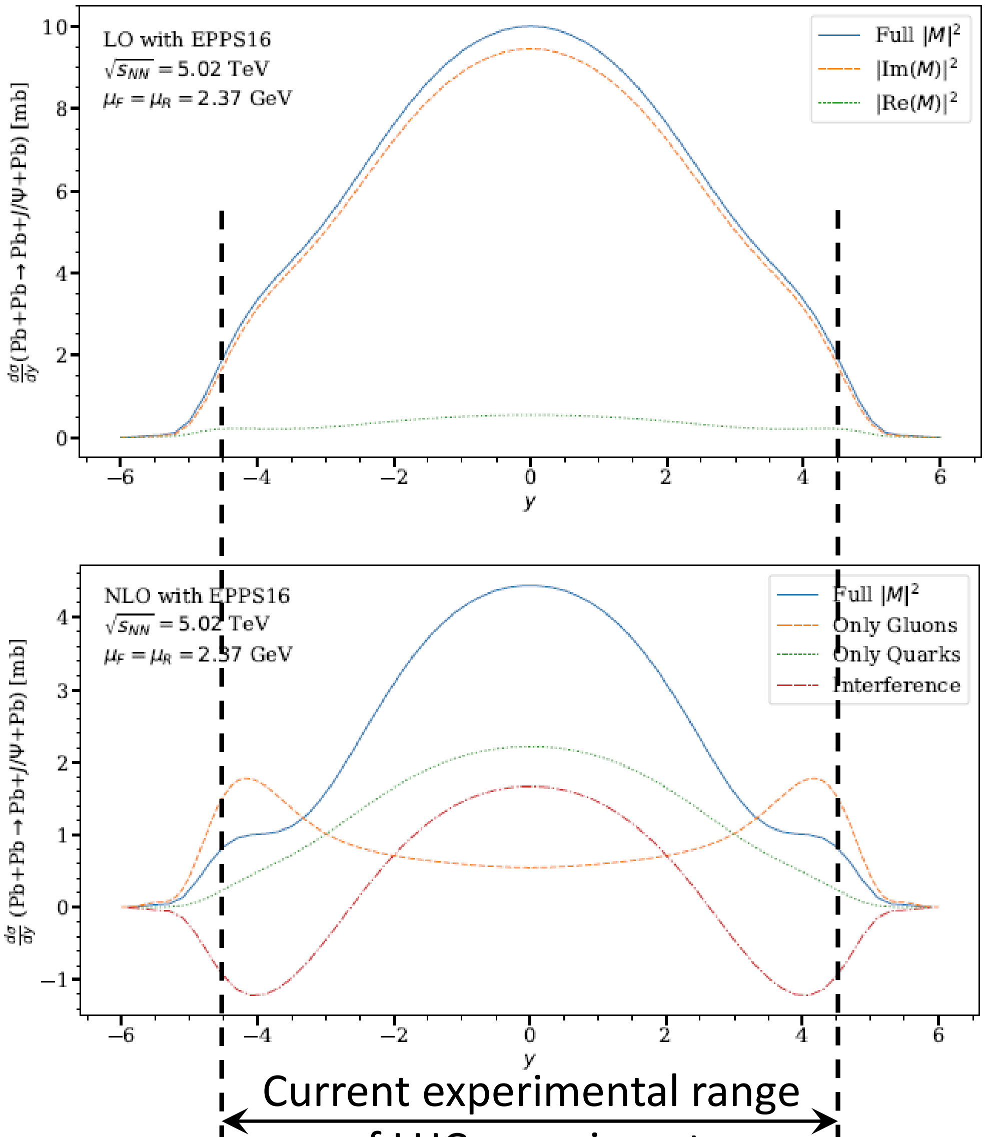

- LO:
  - Gluons
  - Ryskin, Z. Phys. C 57, 89-92 (1993)

$$\frac{d\sigma(\gamma p \to J/\psi p)}{dt} =$$

$$= |F^{2G}{}_N(t)|^2 \frac{\alpha_s{}^2 \Gamma_{ee}{}^J m^3{}_J}{3\alpha_{em}} \pi^3 \left[xG(x,q^2) \frac{2q^2 |q_t{}^J|^2}{(2q^2)^3} \right]^2$$

- NLO:
  - Quarks play a role
  - Eskola et al., Phys. Rev. C 106 (2022) no. 3, 035202; arXiv:2210.16048

$$\mathcal{M} = \mathcal{M}_G^{\mathrm{LO}} + \mathcal{M}_G^{\mathrm{NLO}} + \mathcal{M}_Q^{\mathrm{NLO}}$$

- Differences:
  - Gluons vs quarks
  - Shape
  - Normalization
  - Scale dependence
  - nPDF dependence
- What is the impact of higher order corrections?
- Be carefull with interpretation!

p_T signature

- **Coherent** Vector Meson (VM) photoproduction:
  - Photon couples coherently to all nucleons (whole nucleus)
  - $<p_T^{VM}> \sim 1/R_{Pb} \sim 50$ MeV/c
  - Target ion stays intact
- **Incoherent** VM photoproduction:
  - Photon couples to a single nucleon
  - $<p_T^{VM}> \sim 1/R_p \sim 400$ MeV/c
  - Target ion breaks, nucleon stays intact
  - Usually accompanied by neutron emission
- **Exclusive** VM photoproduction on target proton:
  - Photon couples to a single proton
  - $<p_T^{VM}> \sim 1/R_p \sim 400$ MeV/c
  - Target proton stays intact (similar to coherent) in p-Pb case
- **Dissociative** (or semiexclusive) VM photoproduction:
  - Photon interacts with a single nucleon and excites it
  - $<p_T^{VM}> \sim 1$ GeV/c
  - Target nucleon and ion break (in heavy ion collision)
  - Target proton breaks (in p-Pb)

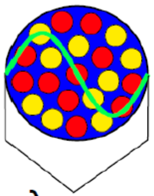

$\lambda_{Coherent}$

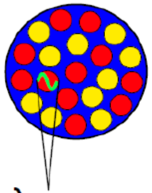

$\lambda_{Incoherent}$

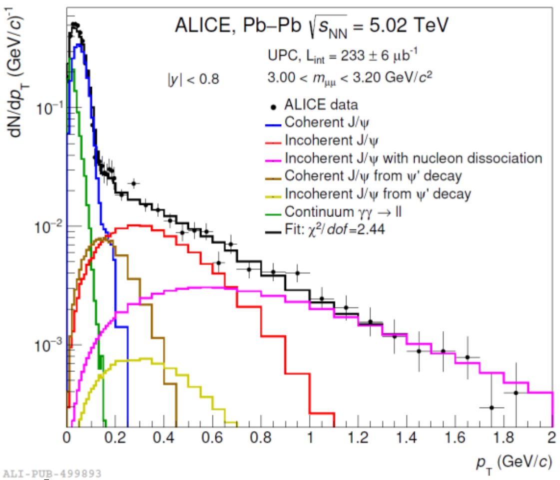

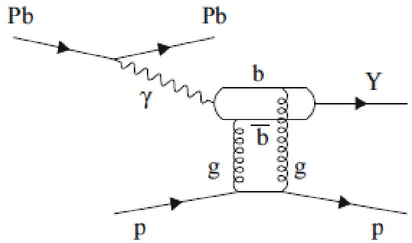

Eur. Phys. J. C (2019) 79:277

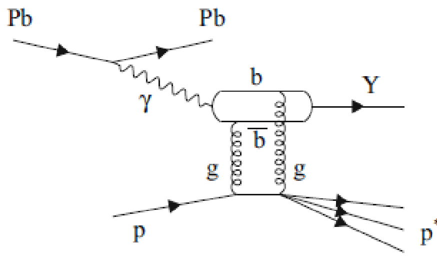

Motivation

- **Coherent** vector meson (ρ^0, J/ψ, $\psi(2S)$) **photoproduction** particularly sensitive to the **gluon shadowing**
  - Nuclear gluon shadowing factor $S_{Pb} = R_g^A(x,Q^2) = g_A(x,Q^2)/Ag_p(x,Q^2) < 1$
  - Saturation may contribute to nuclear shadowing
  - Search for saturation at low x_B
- $|t|$-dependence helps to constrain **transverse gluonic** structure at low x_B
- How well do we model **photon flux**?
- Constrain parameters of **models**
- pQCD test

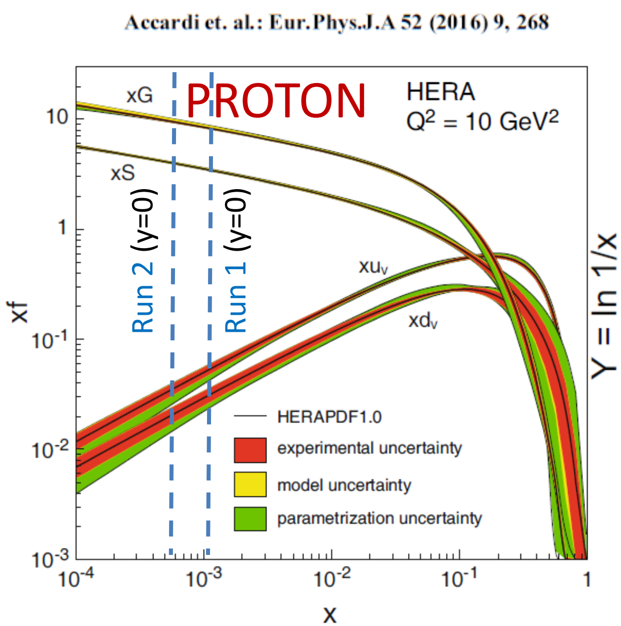

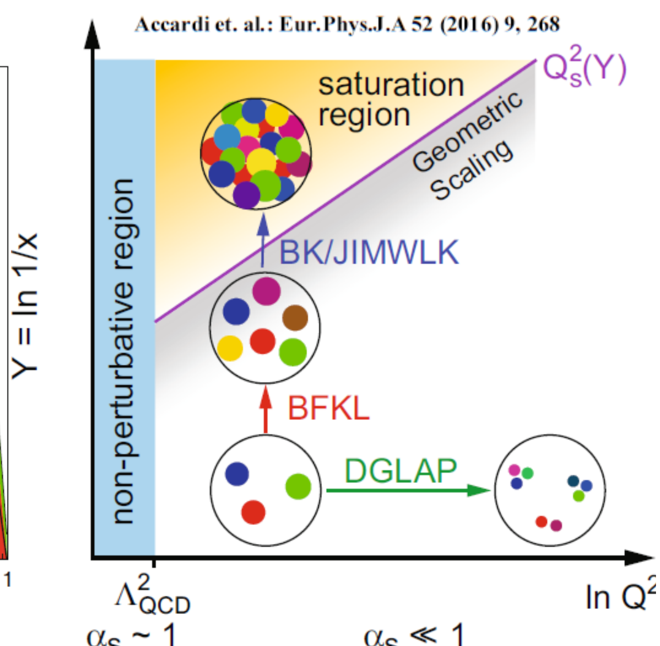

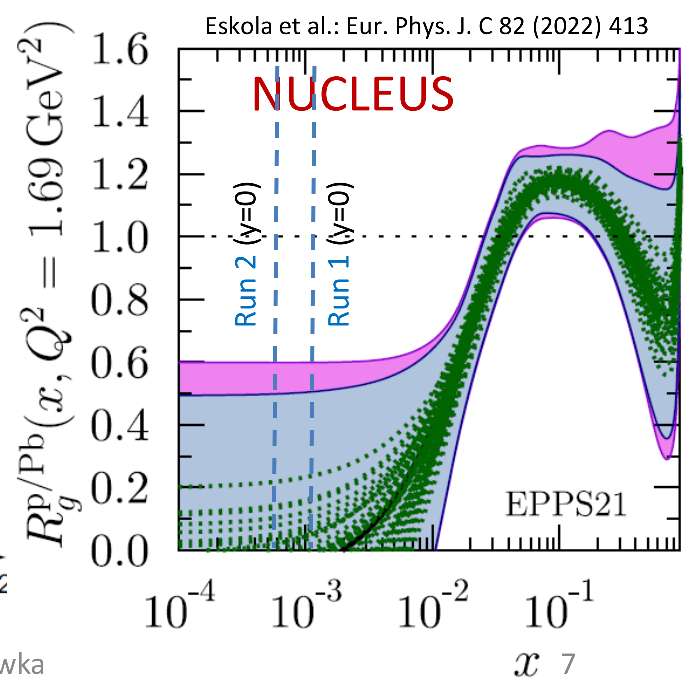

ALICE detector

ALICE: 2008 *JINST* **3** S08002;
Int. J. Mod. Phys. A29 (2014) 1430044

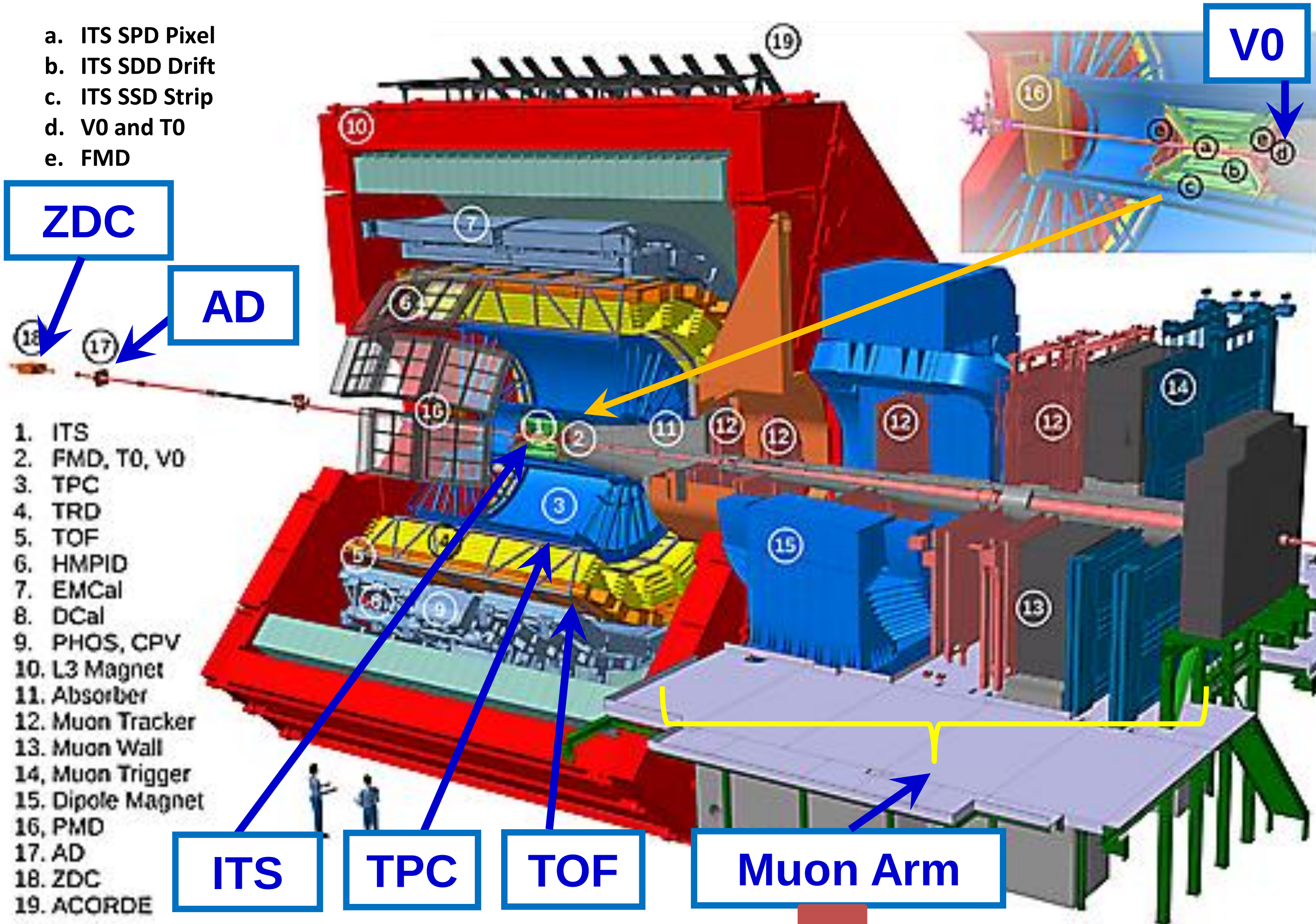

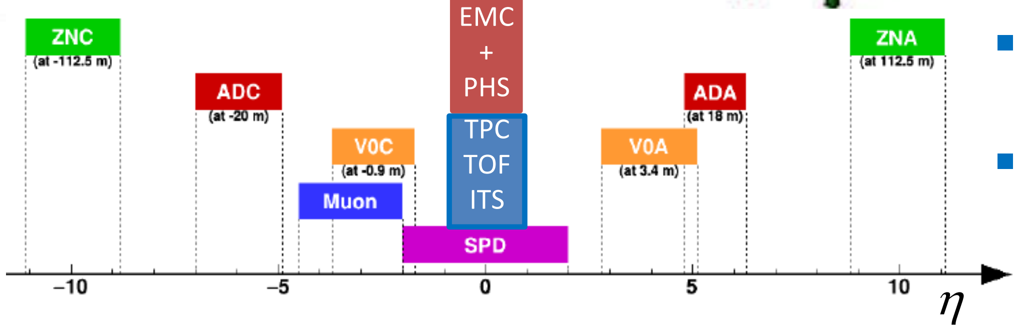

- **Central Barrel tracking ($e^{\pm}$, $h^{\pm}$)**
  – $|\eta| < 0.9$, $0 < \varphi < 2\pi$
  – ITS - silicon detector
  – TPC - gas drift detector
  – TOF - resistive plate chambers
- **Forward tracking ($\mu^{\pm}$)**
  – $-4 < \eta < -2.5$
  – Absorber
  – Muon tracker
  – Muon trigger
  – Dipole magnet
- **Diffractive detectors**
  – AD - scintillator counter
  – V0 - scintillator counter
  – ZDC - sampling calorimeter
- **Vertex**
  – Pixel
- **Trigger**
  – SPD, TOF, AD, V0, Muon

Coherent J/ψ in Pb-Pb at $\sqrt{s_{NN}}$ = 5 TeV

ALICE

- **Wide** rapidity range:
  - **Forward** region: $J/\psi \rightarrow \mu^+\mu^-$
  - **Central** region: $J/\psi \rightarrow \mu^+\mu^-$, e^+e^- and pp
- **Nuclear gluon shadowing factor**
  - $S_{Pb}(y{\sim}0) = \sqrt{\frac{d\sigma}{dy}_{data} / \frac{d\sigma}{dy}_{IA}}$
  - $S_{Pb} = 0.64 \pm 0.04$ for $0.3 \times 10^{-3} < x_B < 1.4 \times 10^{-3}$
- **Compatibility** between ALICE, LHCb and CMS results, but … **tensions** are visible

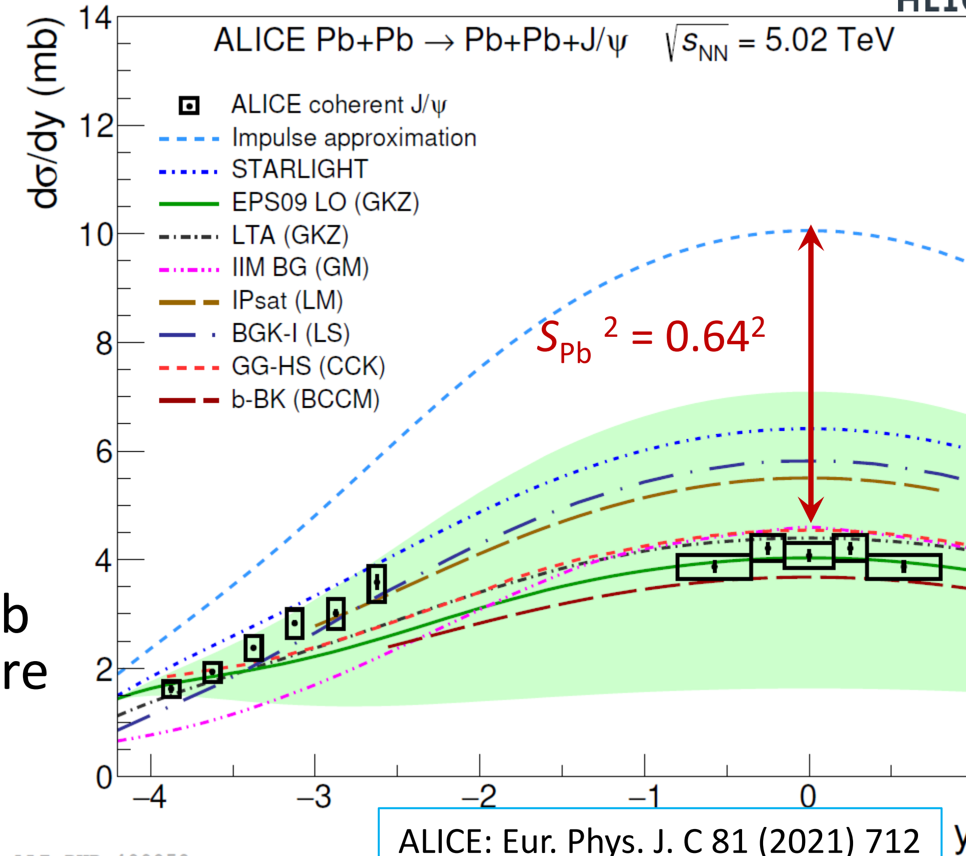

ALICE: Eur. Phys. J. C 81 (2021) 712

- **No model describes the full rapidity dependence**
  - Models with nuclear shadowing (EPS09 LO, LTA) or saturation (GG-HS) describe central and very forward data but tensions in semiforward region
  - Other models describe either (semi-)forward or central rapidity region

Rapidity dependance: Ambiguity problem

- Two sources ⇒ two values of x_B

Eur. Phys. J. C 81 (2021) 712

$$\frac{d\sigma_{AA\to AA'J/\psi}}{dy} = N(\omega_{\gamma 1})\sigma_{\gamma A}(\omega_{\gamma 1}) + N(\omega_{\gamma 2})\sigma_{\gamma A}(\omega_{\gamma 2})$$

High energy photon

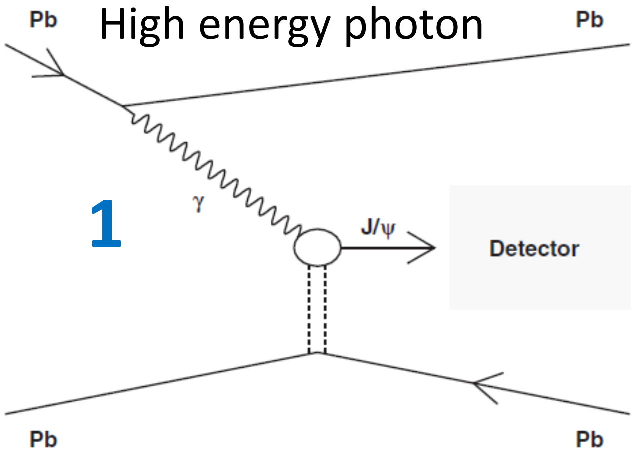

Low energy photon

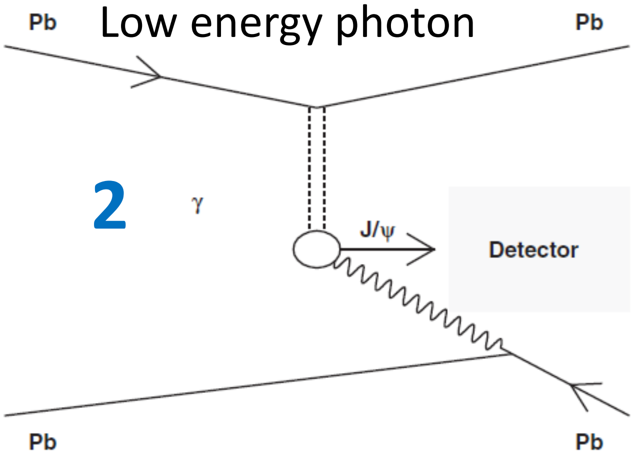

Contreras, PRC 96, 015203 (2017)

$$\omega_{\gamma 1} = \frac{M_{VM}}{2} e^{+y}$$

$$x_B = \frac{1}{\omega_{\gamma 1,\gamma 2}} \frac{M^2{}_{VM}}{2\sqrt{s_{NN}}}$$

$$\omega_{\gamma 2} = \frac{M_{VM}}{2} e^{-y}$$

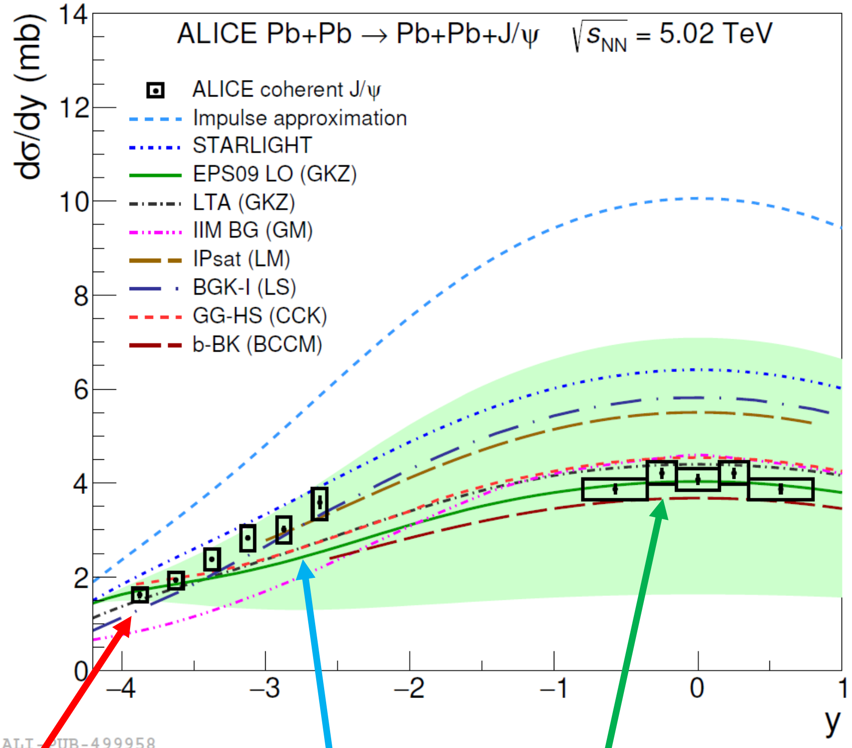

1: 5 % $x_B \sim 1.1 \times 10^{-5}$
2: 95 % $x_B \sim 3.3 \times 10^{-2}$

1: 40 % $x_B \sim 5.1 \times 10^{-4}$
2: 60 % $x_B \sim 0.7 \times 10^{-2}$

50 % each $x_B \sim 10^{-3}$

Solving the ambiguity problem

$$\frac{d\sigma_{AA\to AA'J/\psi}}{dy} = N(\omega_{\gamma 1})\sigma_{\gamma A}(\omega_{\gamma 1}) + N(\omega_{\gamma 2})\sigma_{\gamma A}(\omega_{\gamma 2})$$

Photon flux

Photon energy

Coherent J/ψ at **midrapidity**

- UPC cross section can be directly linked to photonuclear cross section

$$\frac{d\sigma}{dy} = 2N(\omega_{\gamma})\sigma_{\gamma Pb}(\omega_{\gamma})$$

Coherent J/ψ at **forward rapidity**

- 95% of the cross section comes from the low energy photon (high x_B gluon)

$$\frac{d\sigma}{dy} \cong N(\omega_{\gamma 2})\sigma_{\gamma Pb}(\omega_{\gamma 2})$$

To disentangle both photon contributions we need to measure the same proces in peripheral collisions or with EMD!

Coherent J/ψ in non UPC Pb-Pb

- **Low p_T** (< 0.3 GeV/c) and ***R*$_{AA}$ excess** (24σ for the peripheral class) explained by photoproduction in **peripheral** collisions
- Hadroproduction dominates in higher p_T intervals
- Good description of R_{AA} by model (W. Shi et al.) with medium effects + photoproduction. QGP effects also considered
- Both **forward** and **central** region
- Similar observation by LHCb (PRC 105 (2022) L032201)
- Is the same for **other VMs**?

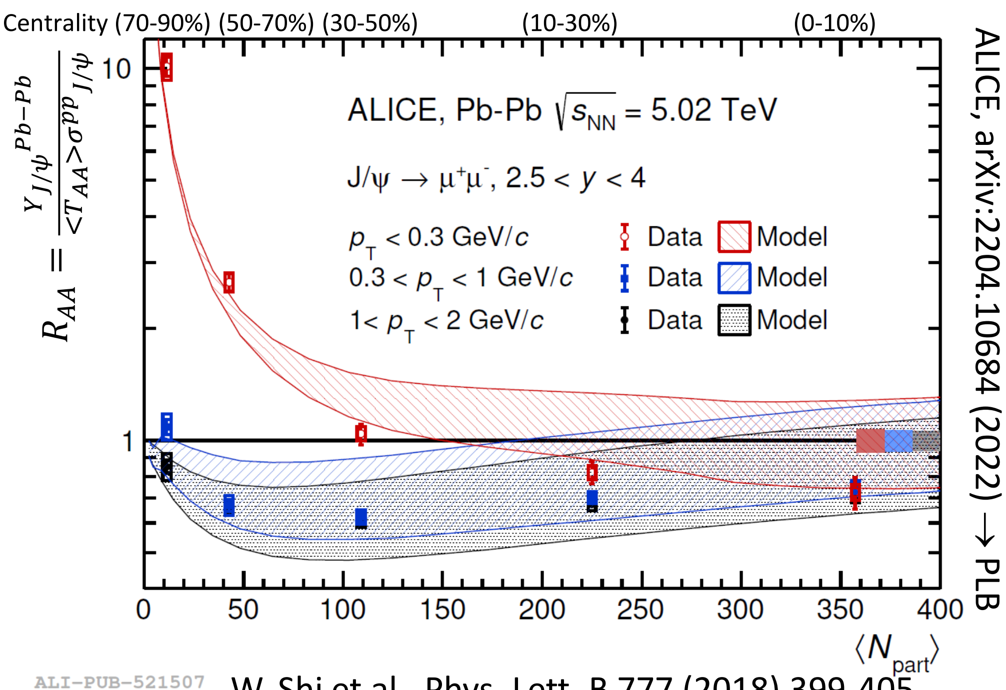

W. Shi et al., Phys. Lett. B 777 (2018) 399-405

Photo-production in peripheral

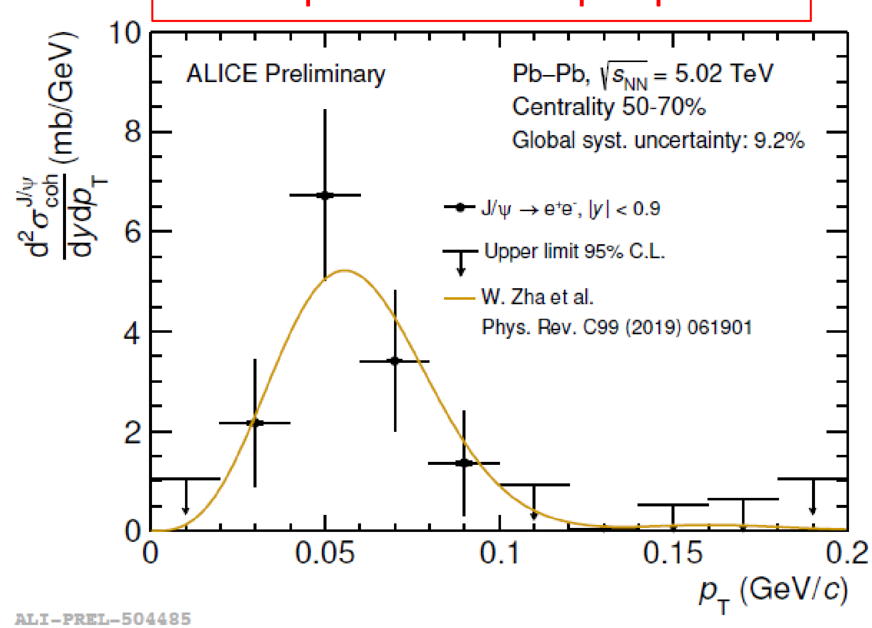

Impact parameter dependence

No breakup (0n0n)

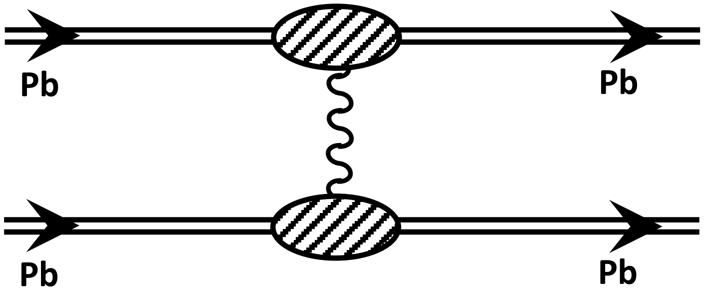

Single breakup (Xn0n + 0nXn)

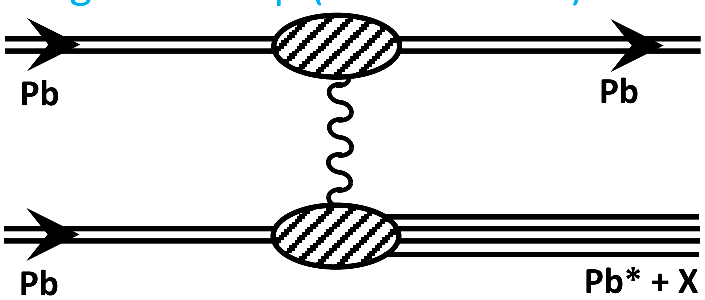

Double breakup (XnXn)

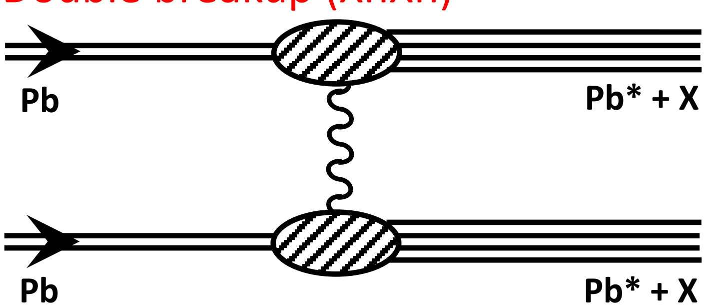

- Excitation of the nuclei possible through the secondary photon exchange

$\Rightarrow$ Giant dipole resonance

All protons vibrating against all neutrons $\rightarrow$ Knocks out neutrons

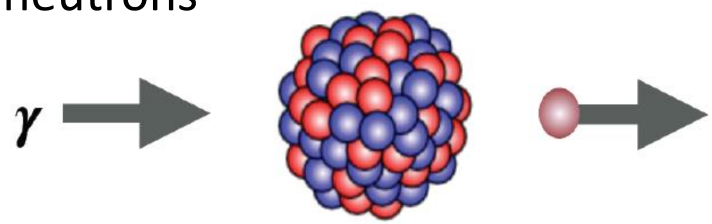

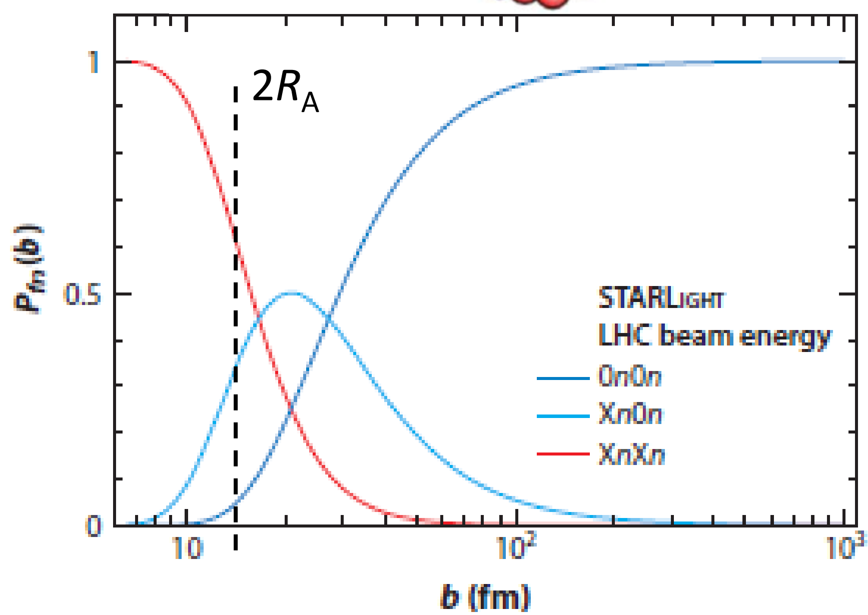

S. Klein, P. Steinberg, Annu. Rev. Nucl. Part. Sci. 70(1), 323 (2020)

UPC event clasifier: 0n0n, 0nXn, XnXn

$\rightarrow$ via electromagnetic dissociation (EMD)

Neutron emission in UPC

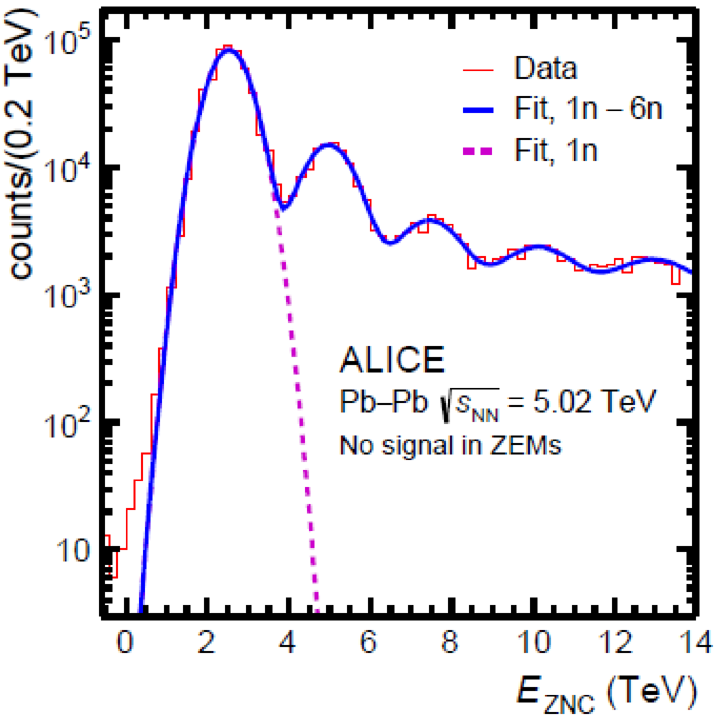

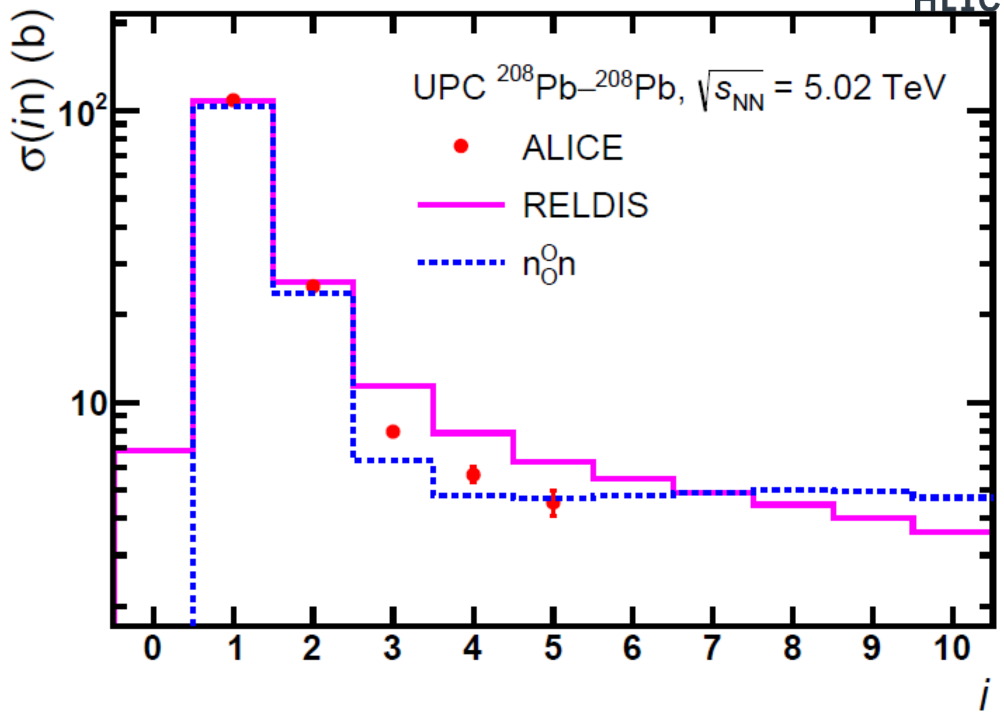

ZN	$\sigma(in)$ (b)	$\sigma^{RELDIS}(in)$ (b)	$\sigma^{n_O^On}(in)$ (b)
1n	$108.4 \pm 0.1 \pm 3.7$	108.0 ± 5.4	103.7 ± 2.1
2n	$25.0 \pm 0.1 \pm 1.3$	25.9 ± 1.3	23.6 ± 0.5
3n	$7.95 \pm 0.04 \pm 0.23$	11.4 ± 0.6	6.3 ± 0.1
4n	$5.65 \pm 0.03 \pm 0.33$	7.8 ± 0.4	4.8 ± 0.1
5n	$4.54 \pm 0.03 \pm 0.44$	6.3 ± 0.3	4.7 ± 0.1
1n–5n	$151.5 \pm 0.2 \pm 4.6$	159.8 ± 5.6	143.1 ± 2.2

- It is huge!
- Up to 5 neutrons
- Hadronic cross section $\sigma_{had} = 7.67 \pm 0.24$ b
- Good description of 1n and 2n emission , but other classes are not so well described

ALICE, arXiv:2209.04250v1 (2022), submitted to PRC

RELDIS: Phys. Part. Nucl. 42 (2011) 215.

N0ON: Comput. Phys. Commun. 253 (2020) 107181.

Techniques to solve the x_B ambiguity

- Different breakup classes using the neutron ZDC on the A and C side
  - Guzey at al., Eur. Phys. J. C 74 (2014) 7, 2942
  - Photon flux depends on the impact parameter
    - Taken from theory, burdened with uncertainties
  - Solving the linear equations resolves the two-fold ambiguity for VMs at y ≠ 0

$$\frac{d\sigma_{PbPb}}{dy} = \frac{d\sigma_{PbPb}{}^{0N0N}}{dy} + 2\frac{d\sigma_{PbPb}{}^{0NXN}}{dy} + \frac{d\sigma_{PbPb}{}^{XNXN}}{dy}$$

$$\frac{d\sigma_{PbPb}{}^{0N0N}}{dy} = N^{0N0N}(\omega_{\gamma1}, +y)\sigma_{\gamma Pb}(\omega_{\gamma1}, +y) + N^{0N0N}(\omega_{\gamma2}, -y)\sigma_{\gamma Pb}(\omega_{\gamma2}, -y)$$

$$\frac{d\sigma_{PbPb}{}^{0NXN}}{dy} = N^{0NXN}(\omega_{\gamma1}, +y)\sigma_{\gamma Pb}(\omega_{\gamma1}, +y) + N^{0NXN}(\omega_{\gamma2}, -y)\sigma_{\gamma Pb}(\omega_{\gamma2}, -y)$$

measured | theory | extracted

- Simulataneously uses UPC and peripheral classes
  - Contreras, PRC 96 (2017) 015203

$$\frac{d\sigma_{PbPb}{}^{P}}{dy} = N^{P}(\omega_{\gamma1}, +y)\sigma_{\gamma Pb}(\omega_{\gamma1}, +y) + N^{P}(\omega_{\gamma2}, -y)\sigma_{\gamma Pb}(\omega_{\gamma2}, -y)$$

$$\frac{d\sigma_{PbPb}{}^{U}}{dy} = N^{U}(\omega_{\gamma1}, +y)\sigma_{\gamma Pb}(\omega_{\gamma1}, +y) + N^{U}(\omega_{\gamma2}, -y)\sigma_{\gamma Pb}(\omega_{\gamma2}, -y)$$

Energy dependence in coherent J/ψ

- Compilation of published results based on ALICE Run 1 data compared to current model calculations
  - Sensitivity to $x_B \sim 10^{-4}$
  - Low x_B described by shadowing and saturation models

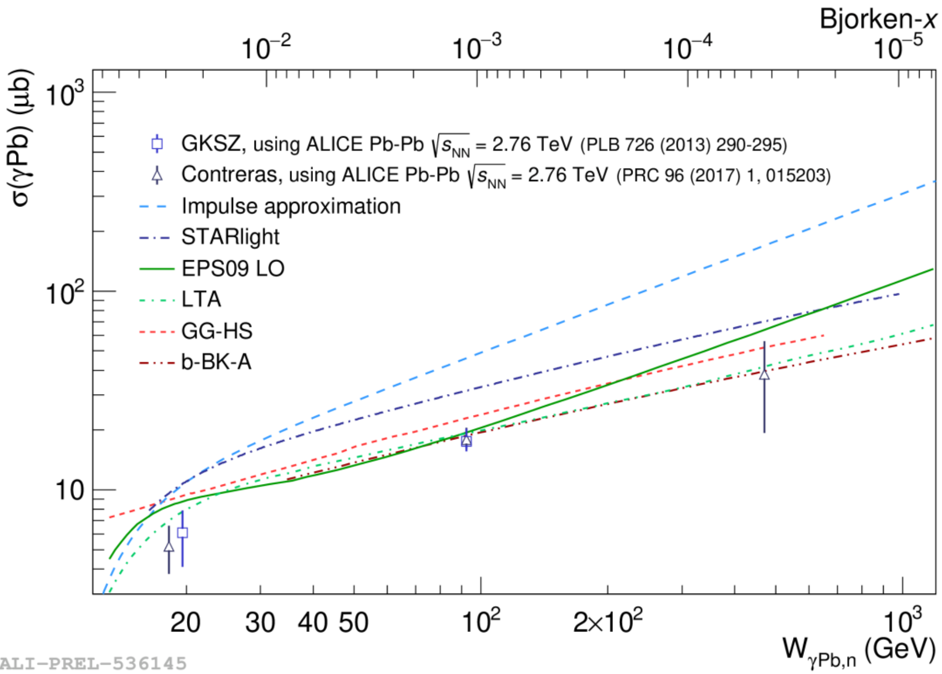

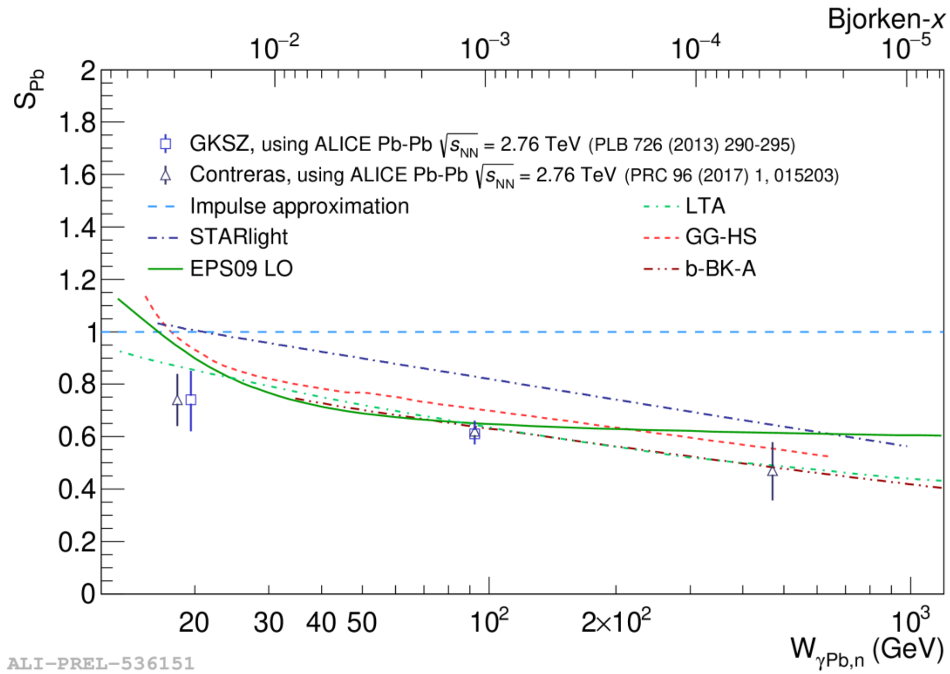

EPS09 LO: PRC 93 (2016) 055206 + JHEP 04 (2009) 065
LTA: PRC 93 (2016) 055206 + Phys. Rept. 512 (2012) 255

GG-HS: PRC97 (2018) 024901
b-BK-A: PLB 817 (2021) 136306

Coherent J/ψ in neutron emission classes

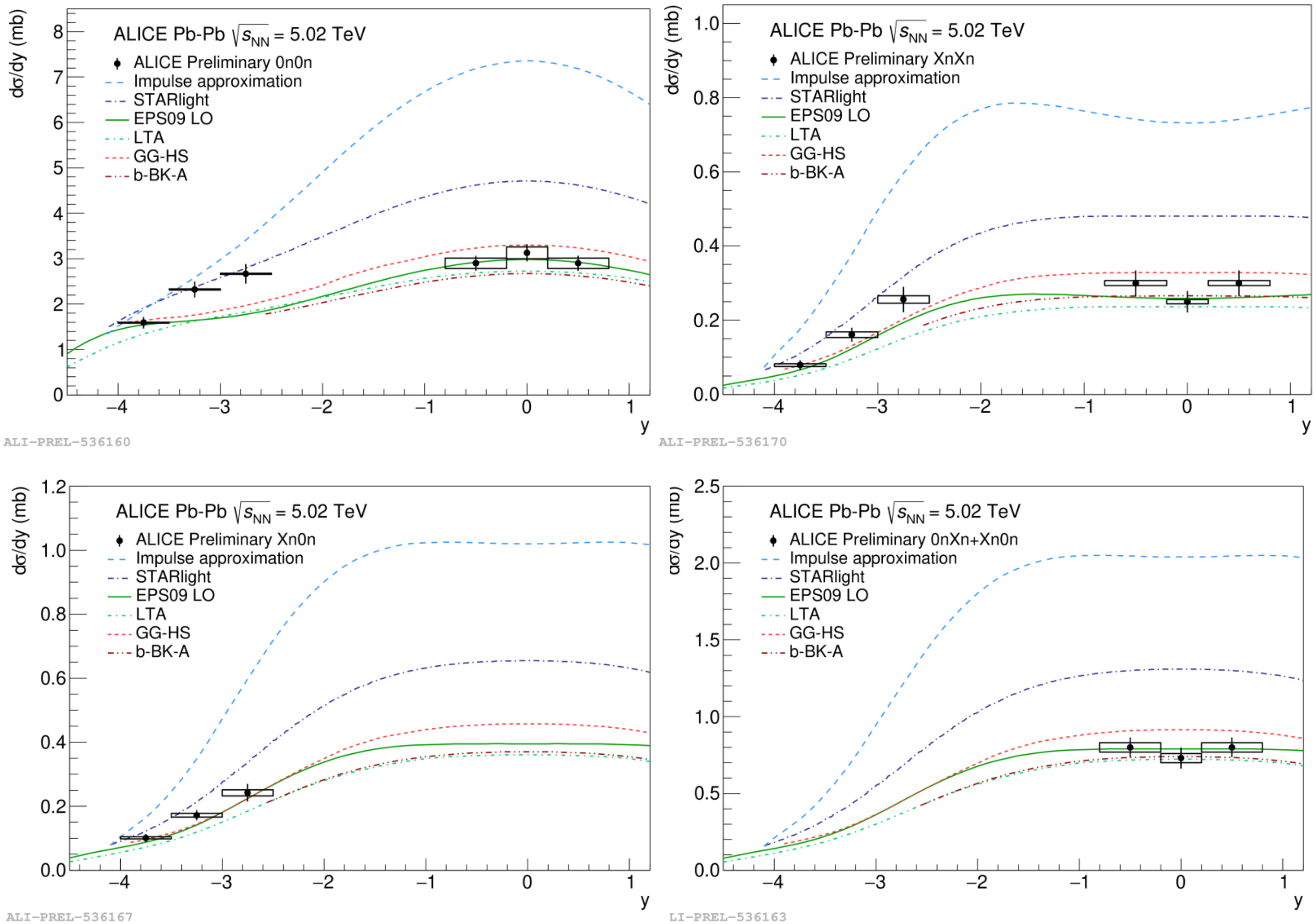

ALICE Run 2

Corrected for:

- Event migration among classes
- Neutrons from pile-up
- Charged particle production from dissociation of either nuclei

Sensitivity to test theoretical models

Good test of photon fluxes

Energy dependence of coherent J/ψ

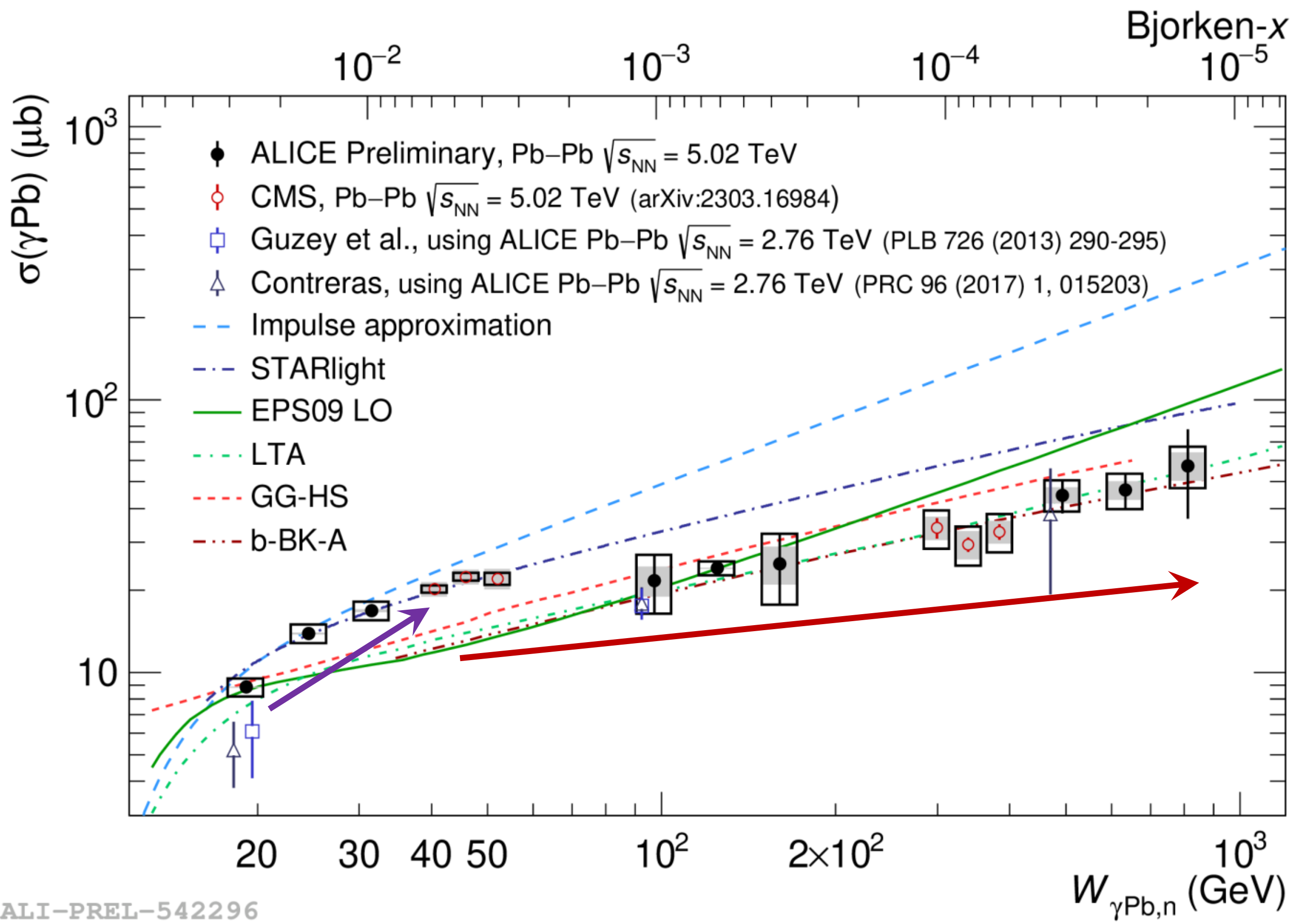

- Rise at low $W_{\gamma Pb,n} \sim$ 15 GeV → ~ 40 GeV

⇒ consistent with fast-growing gluon densities toward lower x_B

- Flattish trend from $W_{\gamma N} \sim$ 40 GeV → ~ 800 GeV

- First measurement of the energy dependence of the photonuclear cross section down to $x_B \sim 10^{-5}$
- Consistency between two methods: Run 1 with peripheral collisions and Run 2 data with neutron emission classes
- Neutron emission technique extends the explored energy range over 300 GeV!
- Unprecedented x_B region is probed, not available by any other LHC experiment
- Both saturation and shadowing models are favored at low-x_B

Nuclear suppression factor of coh. J/ψ

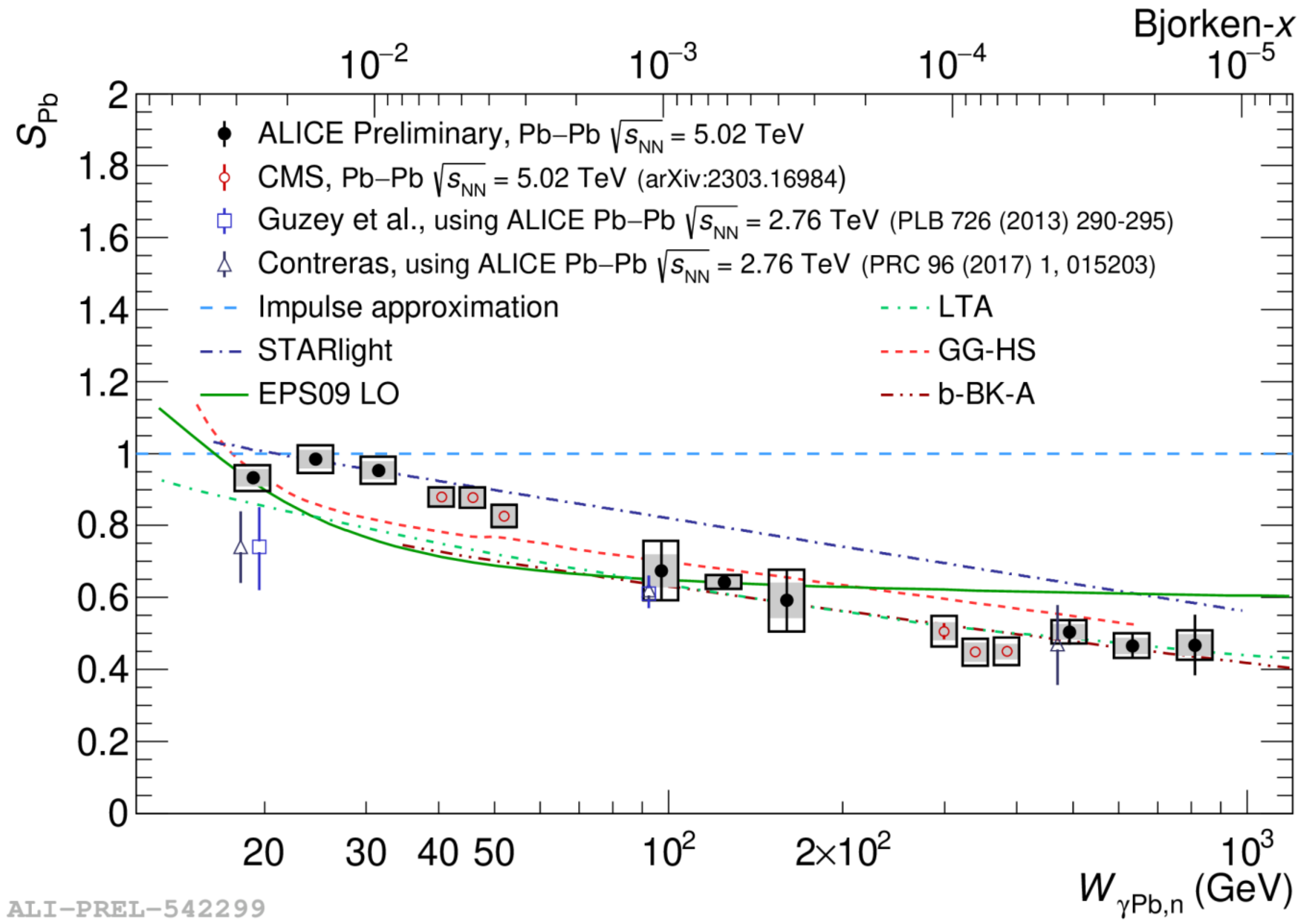

- First measurement of the nuclear suppression factor down to $x_B \sim 1.1 \times 10^{-5}$
- Very wide energy range 20 – 800 GeV
- At low-x_B data favours both saturation and shadowing models
- Additional uncertainty from impulse approximation

No model describes the whole energy/Bjorken-*x* range!

Coherent ψ(2S) photoproduction

- UPC Pb-Pb at $\sqrt{s_{NN}}$ = 5.02 TeV
- $\psi(2S) \rightarrow \mu^+\mu^-\pi^+\pi^-$, $e^+e^-\pi^+\pi^-$, l^+l^-
- **Nuclear gluon shadowing factor**
  - $S_{Pb} = 0.66 \pm 0.06$ for $0.3 \times 10^{-3} < x_B < 1.4 \times 10^{-3}$
  - Consistent with J/ψ result
- Good agreement of **models with shadowing** (EPS09 LO, LTA, Guzey et al.)
- Good agreement of ALICE data with model BCCM (with saturation)
- Other models overpredict ALICE data

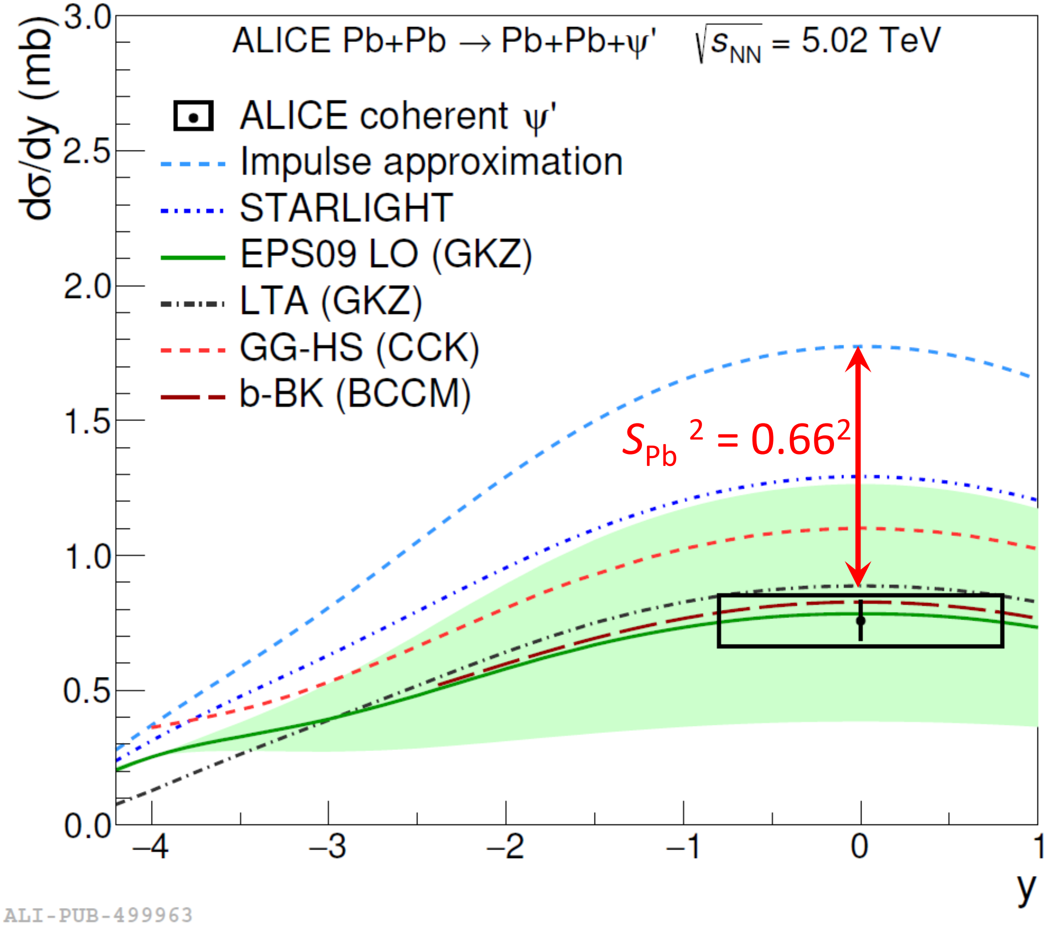

ALICE, Eur. Phys. J. C 81 (2021) 712

Coherent vs. Incoherent J/ψ in γp

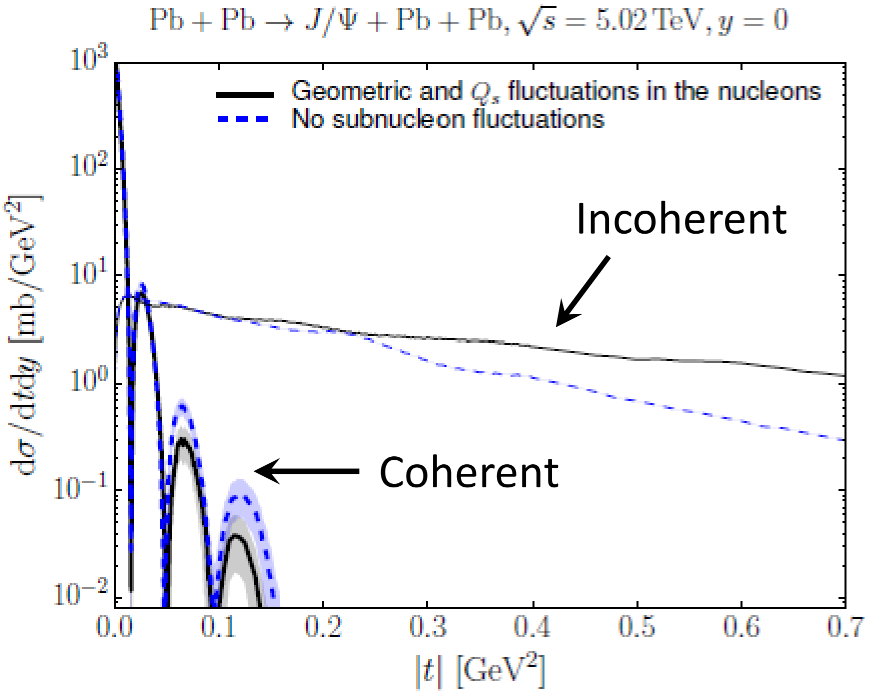

Mantysaari, Schenke, PLB 772 (2017) 832

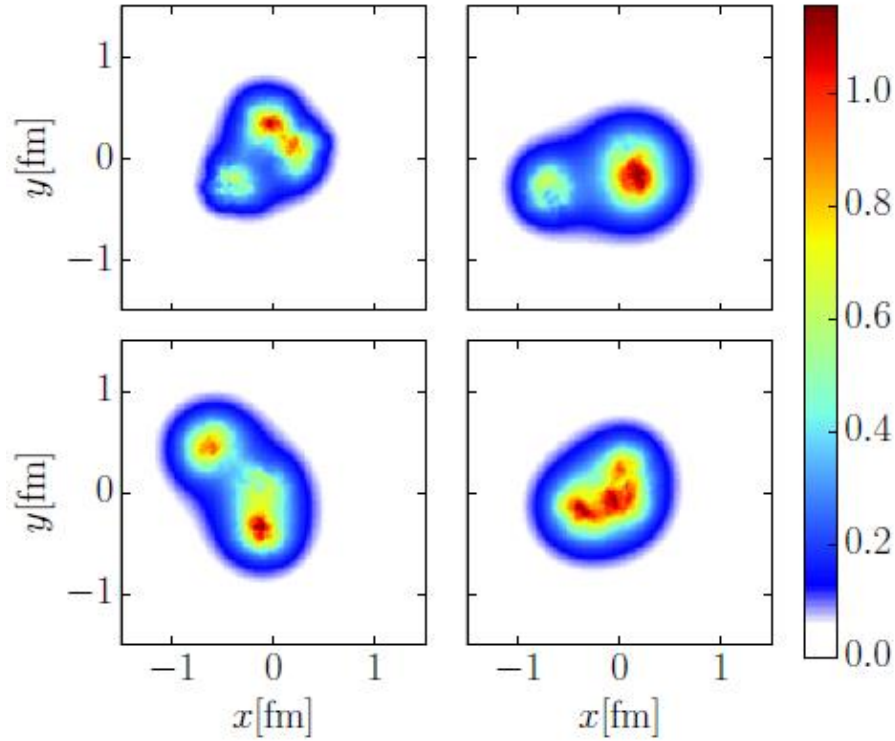

Event by event fluctuations of proton density profile
Mantysaari, Schenke, PRD 94 (2016) 034042

- Wider |t|-distribution → scatter of smaller object
- Variations → quantum fluctuations
- Fluctuations = subnucleon degrees of freedom
- Are subnucleon dof. significant?

Coherent J/ψ

- Central region
  - $J/\psi \rightarrow \mu^+\mu^-$
- Coherent $|t|$ **dependence** is sensitive to the average spatial gluon distribution
- Bayesian and SVD unfolding used to transform $p_T^2 \rightarrow |t|$
- Transition from UPC to photonuclear cross section

Photon flux

$$\left.\frac{d^2\sigma^{coh}_{J/\psi}}{dy\,dp_T^2}\right|_{y=0} = 2n_{\gamma Pb}(y=0)\,\frac{d\sigma_{\gamma Pb}}{d|t|}$$

- Comparison to models:
  - STARlight does not contain explicitly shadowing – do not describe shape nor magnitude
  - LTA contains nuclear shadowing – agrees with data
  - b-BK based on gluon saturation – agrees with data

ALICE, PLB 817 (2021) 136280

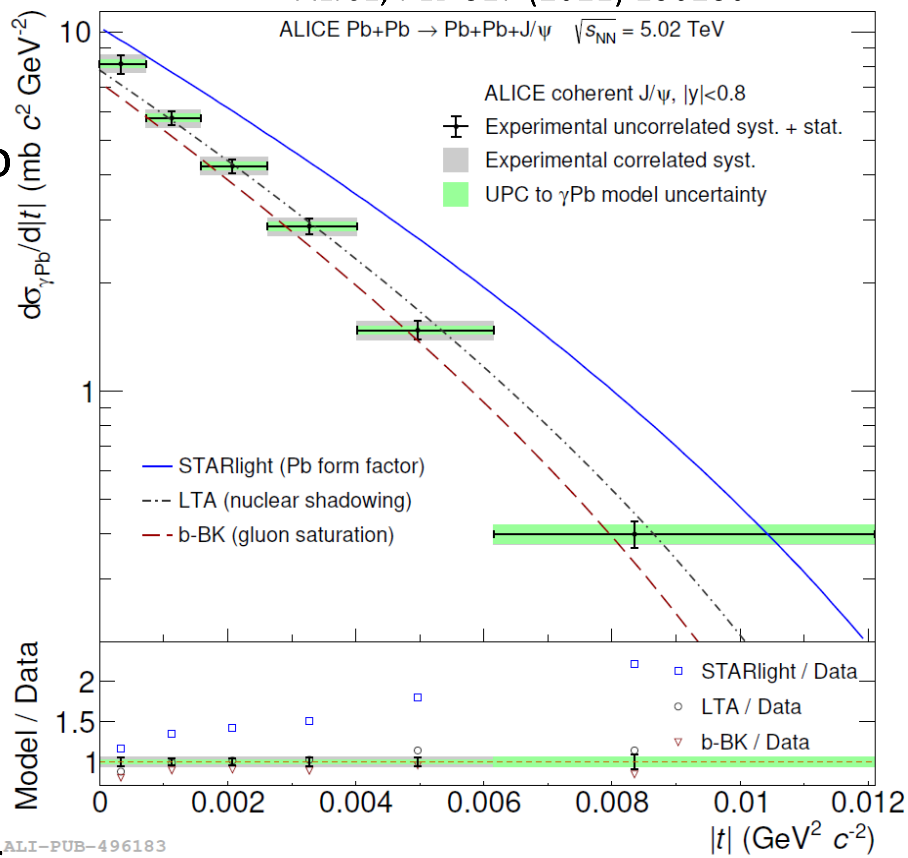

LTA: Phys. Rev. C 95 (2) (2017) 025204.
b-BK: arXiv:2006.12980 [hep-ph].

Incoherent J/ψ

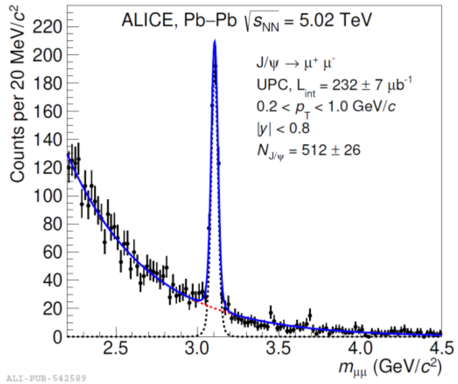

- Central region
  - $J/\psi \rightarrow \mu^+\mu^-$
- Incoherent **|*t*|dependence** is sensitive to the variance of the spatial gluon distribution
- First measurement of this kind ever → probing for gluonic „hot spots" in Pb
- Models fail to predict the normalisation
- Normalization is linked to the scaling from proton to nuclear targets
- (Slope of) data favor models with gluonic subnucleon fluctuations (MS-hs and GSZ el+dis)

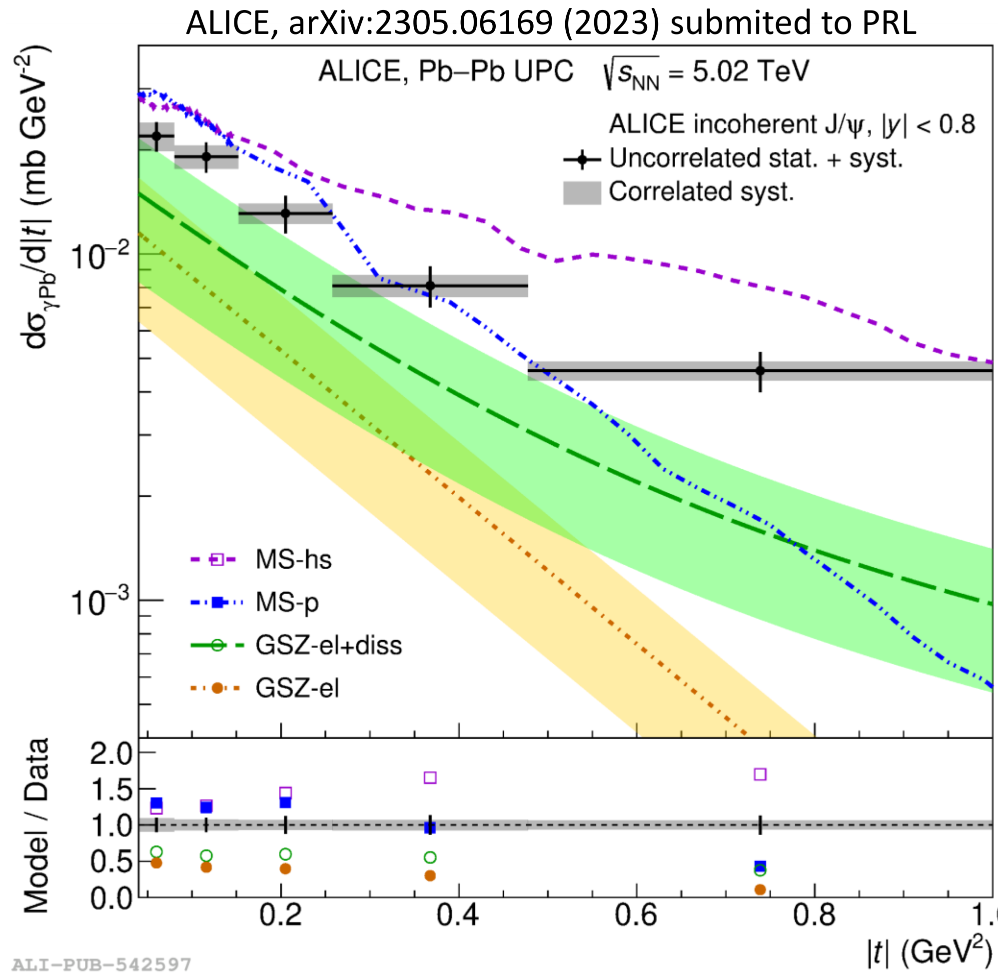

MS (saturation): PLB 772 (2017) 832.
GSZ (shadowing): PRC 99 (2019) 015201.

$\gamma\gamma \rightarrow \mu\mu$ in p-Pb at $\sqrt{s_{NN}}$ = 8.16 TeV

- **$\gamma\gamma \rightarrow \mu\mu$ cross section**
- Good agreement of simulation and data
- Comparison with STARlight and SuperChic (both LO QED, no FSR) shows slight excess in data, but still agreement within 3σ
- Important background for other UPC processes
- Constrains theoretical models

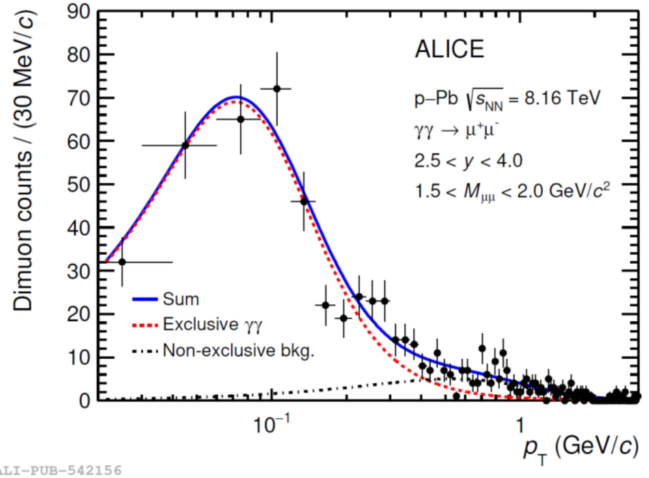

arXiv:2304.12403, submitted to PRD

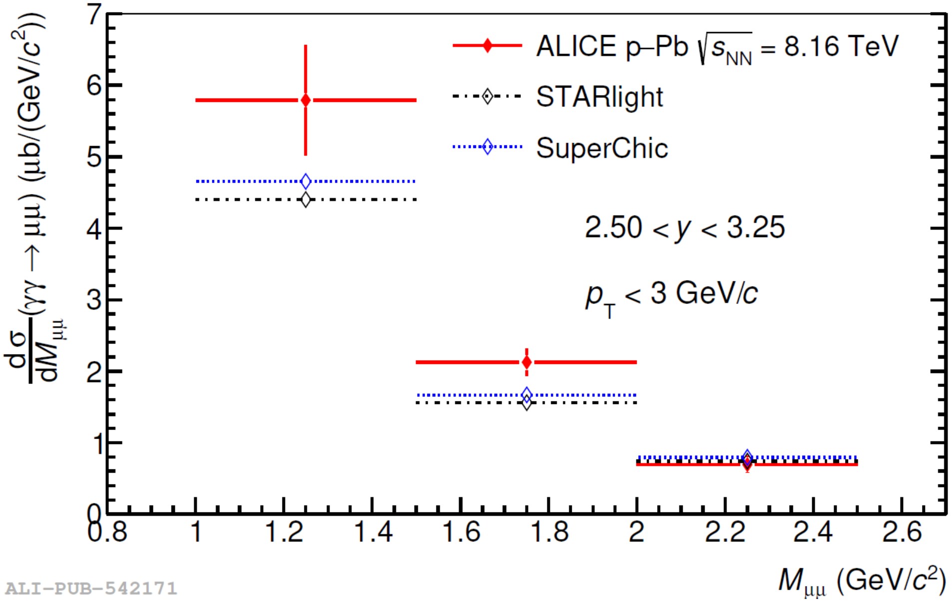

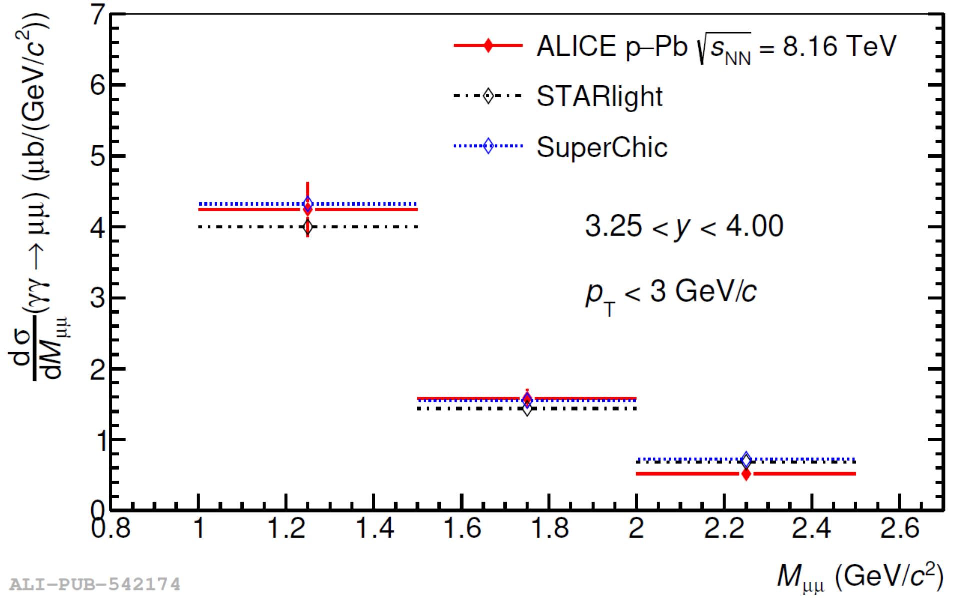

STARlight 2.2.0: Comput. Phys. Commun. 212 (2017) 258.
SuperChic 4.15: EPJC80 (2020) 925.

Photonuclear J/ψ cross section

- Gluon distribution at HERA energies follows power law at low x_B
  $\Rightarrow$ similar trend in $W_{\gamma p}$
- **Exclusive J/ψ cross section** at LHC follows HERA trend so far

ALICE: p-Pb at $\sqrt{s_{NN}}$ = 5.02 and 8.16 TeV
LHCb: pp at $\sqrt{s}$ = 7 and 13 TeV

- Power law fit $\sigma \sim W_{\gamma p}{}^{\delta}$
  - H1 data: $\delta = 0.67 \pm 0.03$
  - ALICE data: $\delta = 0.7 \pm 0.04$
  - $\Rightarrow$ agreement LHC and HERA
  - $\Rightarrow$ agreement ALICE and LHCb
- Models show agreement
  - JMRT NLO: based on DGLAP evolution with dominant NLO contribution
    - valid to $x_B \sim 2 \times 10^{-5}$
  - CCT: Saturation in the energy dependent hot spot model
- Probe wide region $x_B \sim 10^{-2}$ - 10^{-5}

ALICE p-Pb 8.16 TeV: arXiv:2304.12403, submited to PRD, NEW!
ALICE p-Pb 5.02TeV: Phys. Rev. Lett. 113 (2014) 232504.

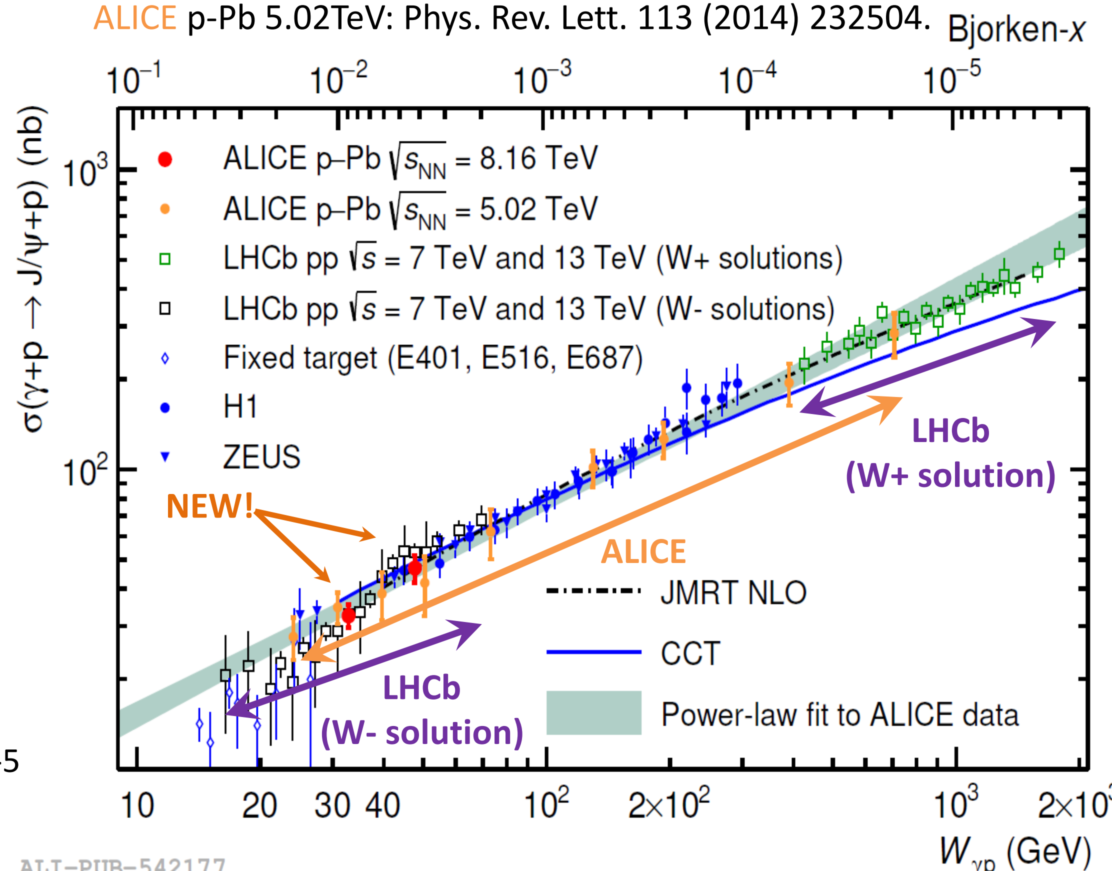

No clear indication of gluon saturation at low x_B

Dissociative J/ψ in p-Pb at $\sqrt{s_{NN}}$ = 8.16 TeV

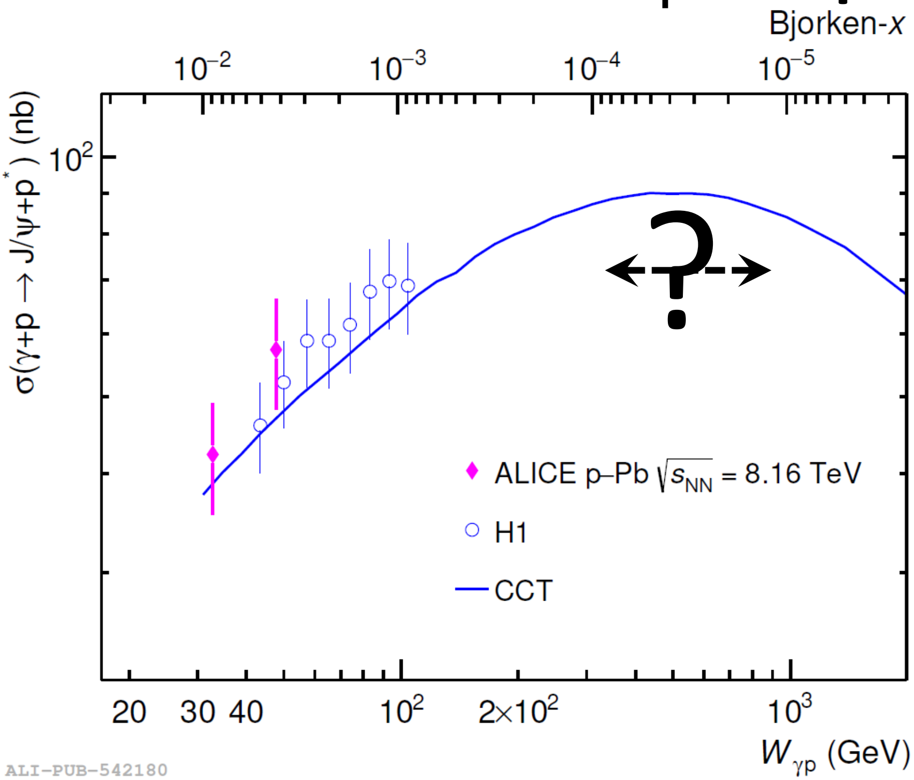

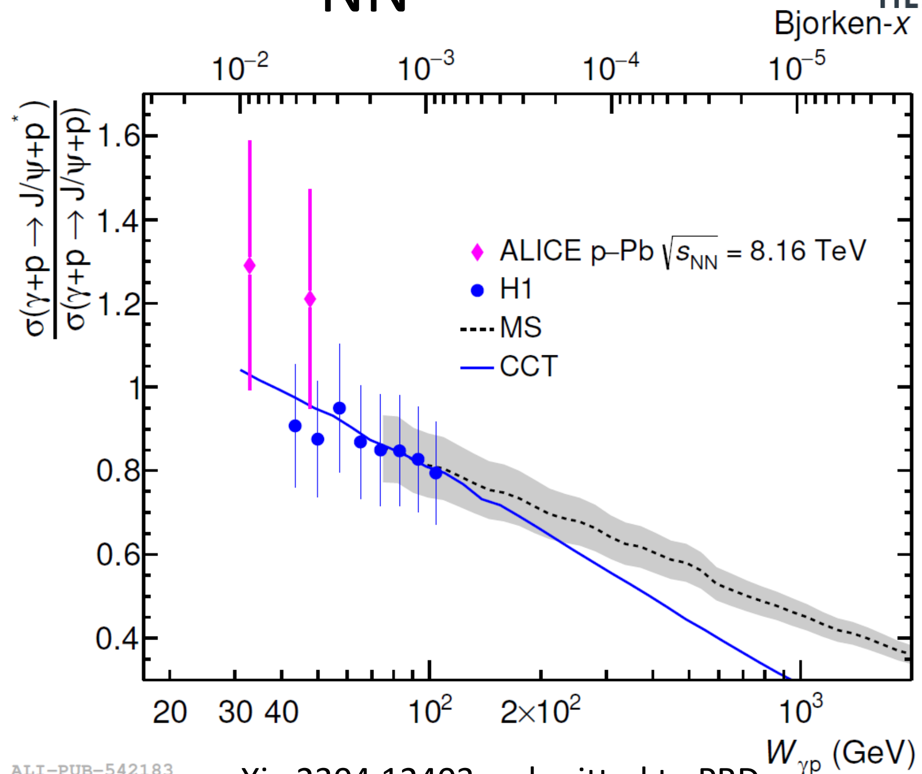

arXiv:2304.12403, submitted to PRD

- **First measurement** of the dissociative cross section at the LHC
- Energy dependent **dissociative J/ψ cross section** (x_B ~ (0.5,2) × 10^{-2})
- Agreement with HERA results (H1, EPJC 73 (2013) 6,2466)
- CCT model with saturation (PLB766 (2017) 186) agrees with data
  - Predicted maximum at $W_{\gamma p}$ ~ 500 GeV to be checked in Run 3
- MS (PRD 98, 3 (2018) 034013) to be checked in Run 3

ρ^0 photoproduction

ALICE, JHEP 06 (2020) 035

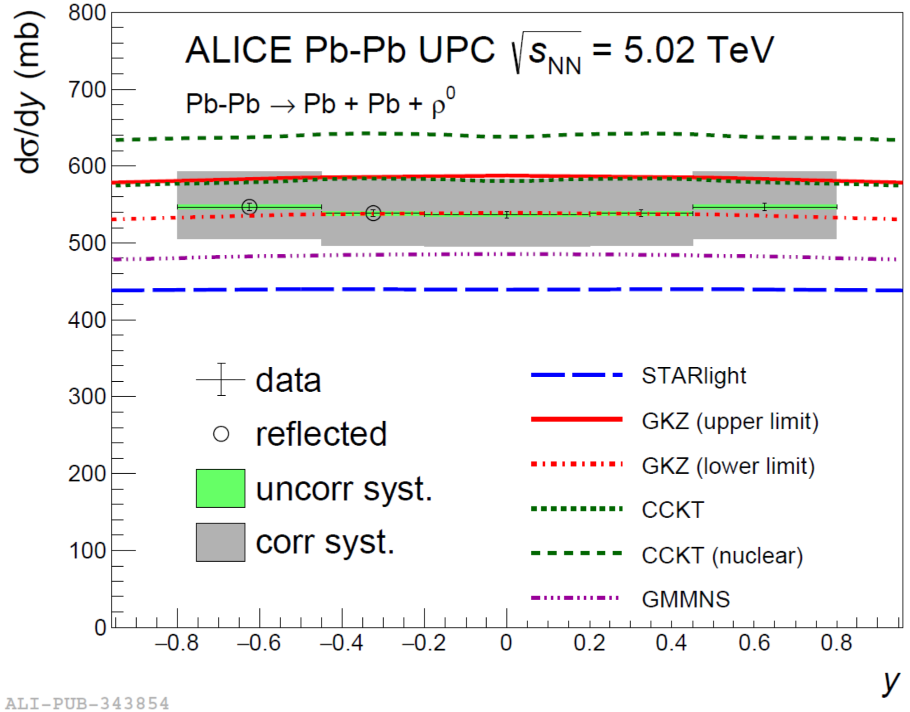

ALICE, Phys. Lett. B 820 (2021) 136481

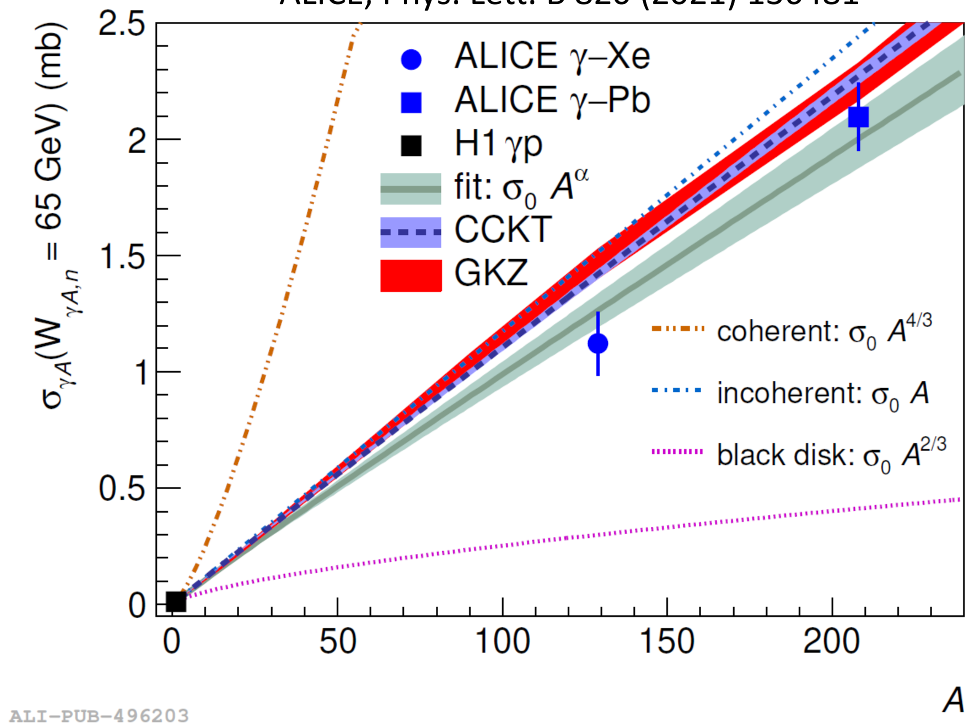

- **Large cross section** (~550 mb) quite well described by models
- Measurement in nuclear **breakup classes** (0n0n, 0nXn, XnXn) to distinguish *b* dependence
- $\sigma(\gamma A \rightarrow \rho^0 A) \sim A^\alpha$ with a slope
  $\alpha = 0.96 \pm 0.02^{sy}$

  ⇒ Signals important **shadowing effect**
- Far away from Black Disk Limit

ρ^0 in Pb-Pb at $\sqrt{s_{NN}}$ = 5.02 TeV

ALICE

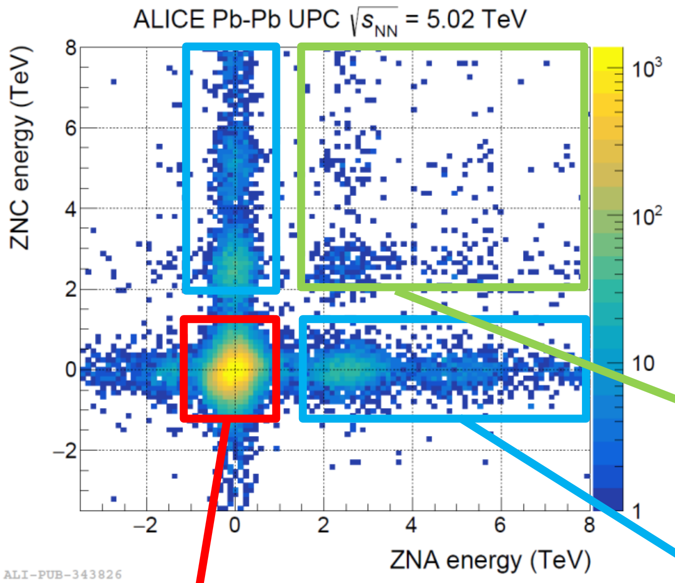

- Impact parameter dependence via ZDC selection in 3 classes: 0n0n, 0nXn, XnXn
- Comparisons with models
  - GKZ (nuclear shadowing) gives the best description
  - CCKT (saturation) is slightly worse
  - STARlight and GMMNS (saturation) underestimate
  - Worst description for 0nXn class
- Test of photon flux description

ALICE: JHEP 06 (2020) 035

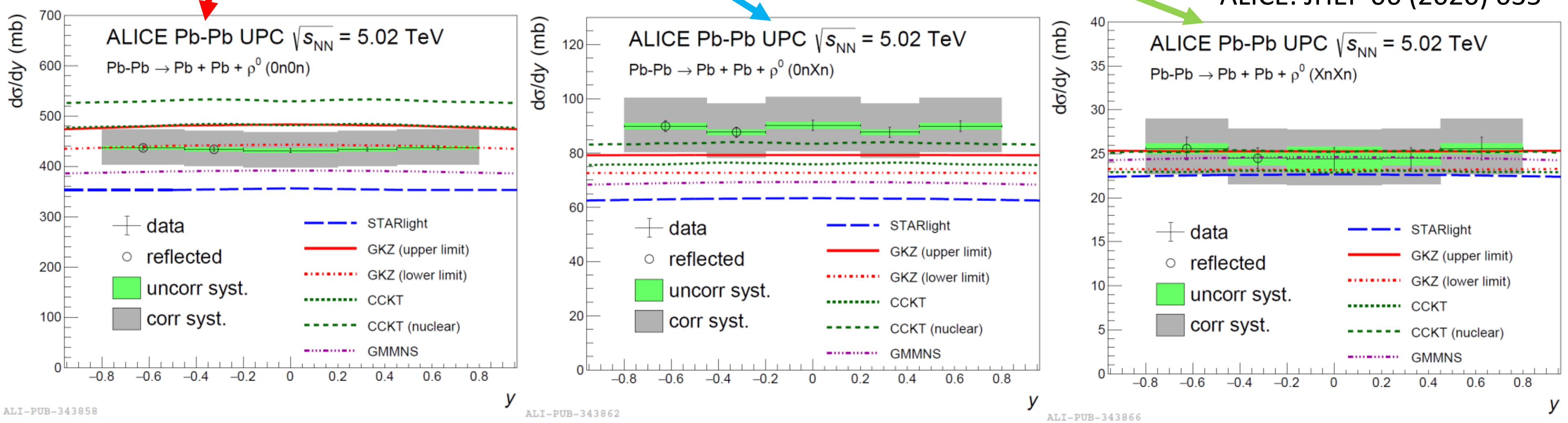

ρ' in Pb-Pb at $\sqrt{s_{NN}}$ = 5.02 TeV

- Resonance-like structure $M^{\pi\pi}$ ~ 1.7 GeV/c^2
  - Significance of 4.5 σ
  - Seen also by STAR, ZEUS, H1
  - Most probably $\rho_3(1690)$ with angular momentum J = 3
  - More data from Run3 + Run4 needed

$$\frac{dN_{\pi\pi}}{dm} = P_1 \cdot \exp(-P_2 \cdot (m - 1.2\,\mathrm{GeV}/c^2)) + P_3 + P_4 \cdot \exp(-(m - M_x)^2/\Gamma_x^2)$$

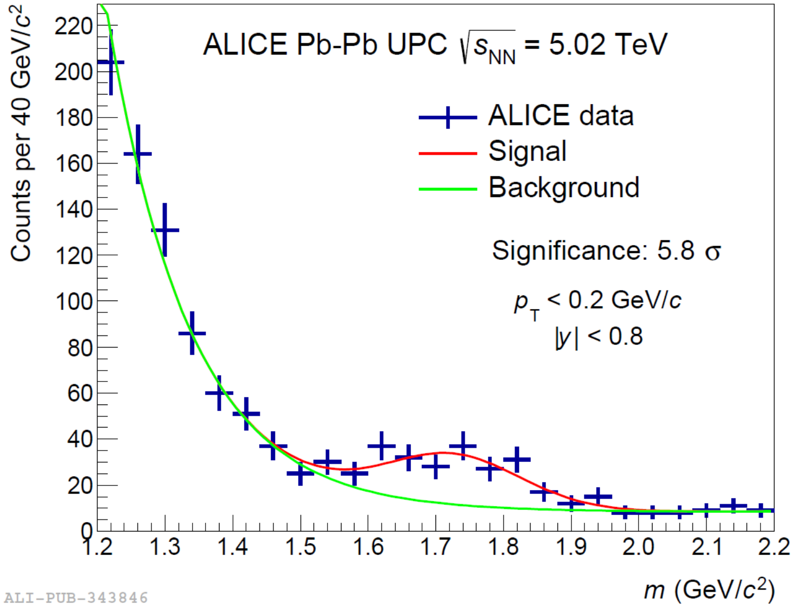

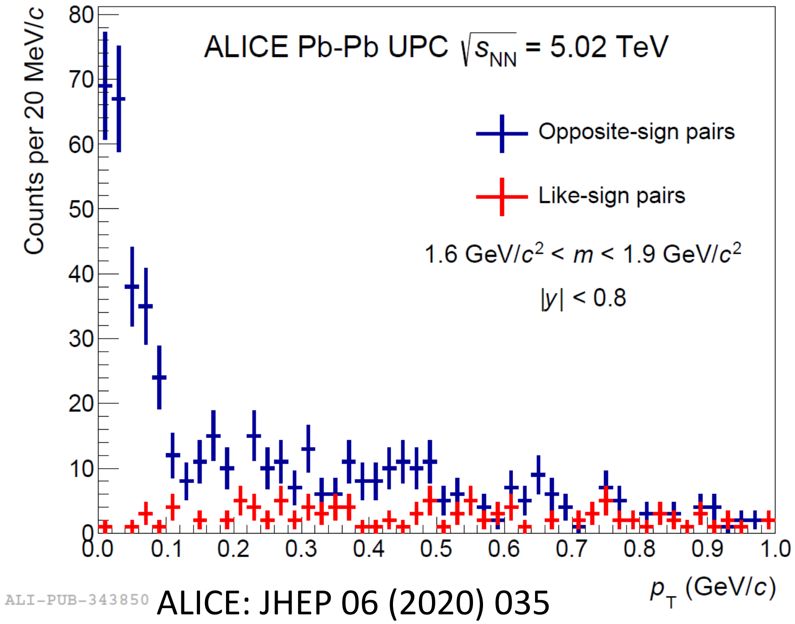

ALICE: JHEP 06 (2020) 035

ALICE 2 vs ALICE 3

ALICE in Run 3 + 4 (2022 - 2032†)

†FoCal upgrade before Run 4

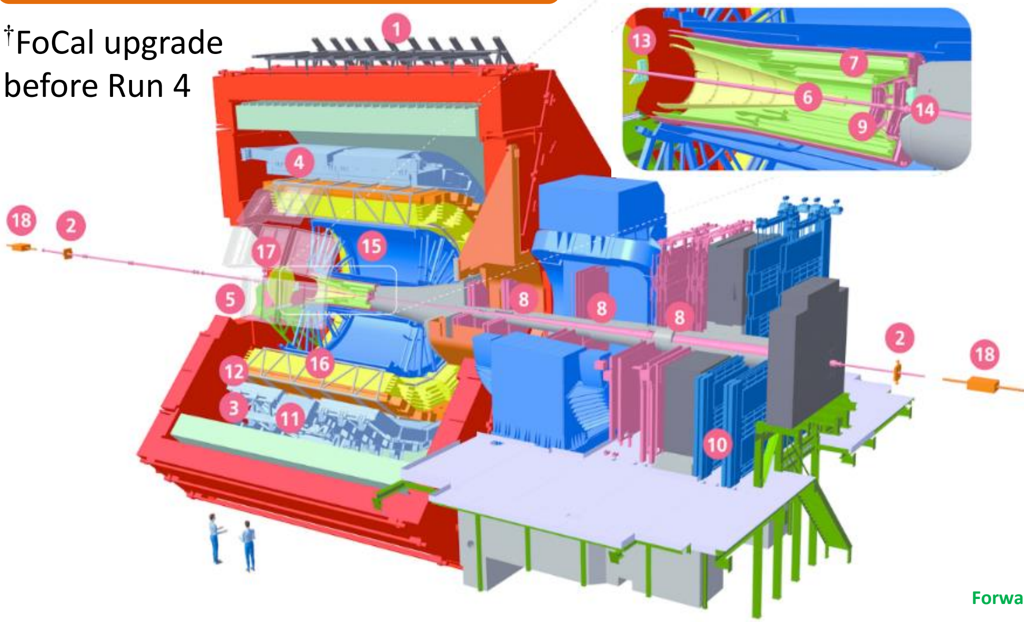

ALICE 3 detector in Run 5 (2035 - 2038)

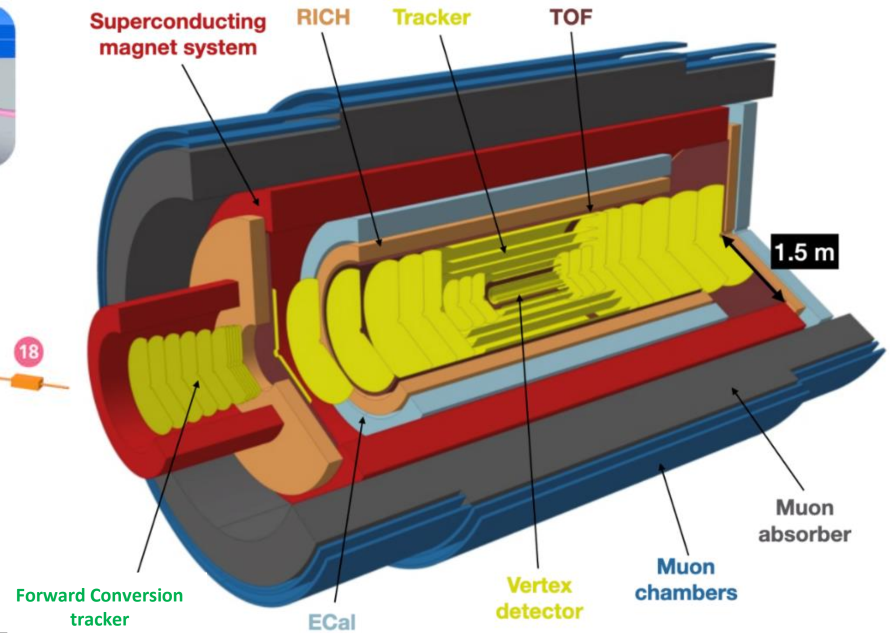

Adamova *et al.*, 1902.01211 (2019); CERN-LHCC-2022-009

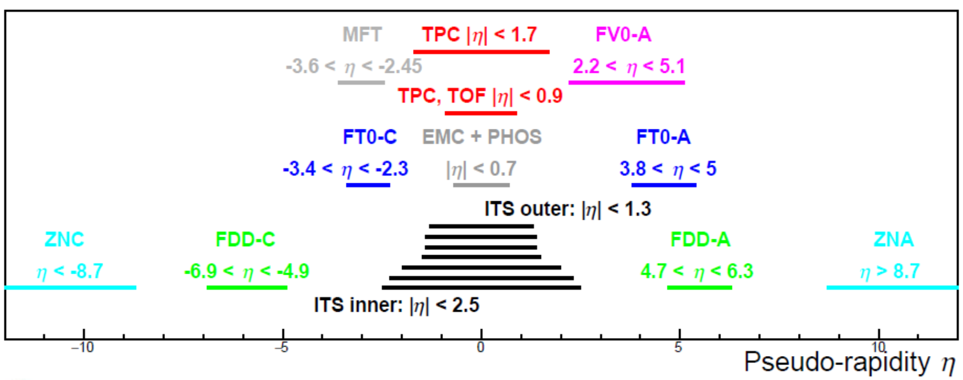

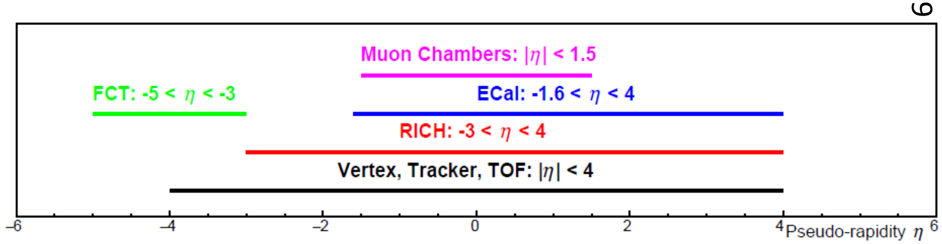

1 **ACORDE** | ALICE Cosmic Rays Detector
2 **AD** | ALICE Diffractive Detector
3 **DCal** | Di-jet Calorimeter
4 **EMCal** | Electromagnetic Calorimeter
5 **HMPID** | High Momentum Particle Identification Detector
6 **ITS-IB** | Inner Tracking System - Inner Barrel
7 **ITS-OB** | Inner Tracking System - Outer Barrel
8 **MCH** | Muon Tracking Chambers
9 **MFT** | Muon Forward Tracker
10 **MID** | Muon Identifier
11 **PHOS / CPV** | Photon Spectrometer
12 **TOF** | Time Of Flight
13 **T0+A** | Tzero + A
14 **T0+C** | Tzero + C
15 **TPC** | Time Projection Chamber
16 **TRD** | Transition Radiation Detector
17 **V0+** | Vzero + Detector
18 **ZDC** | Zero Degree Calorimeter

ALICE in future runs (3, 4 and beyond)

- Precise and new vector meson photoproduction
- Light-by-light scattering
- $(g-2)_\tau$

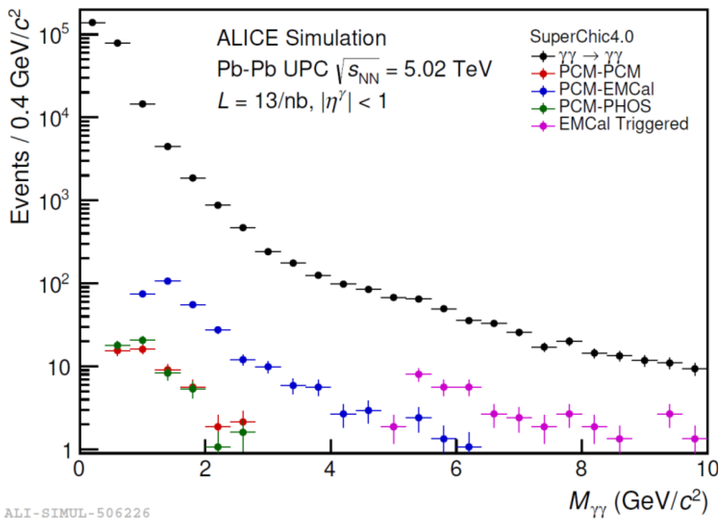

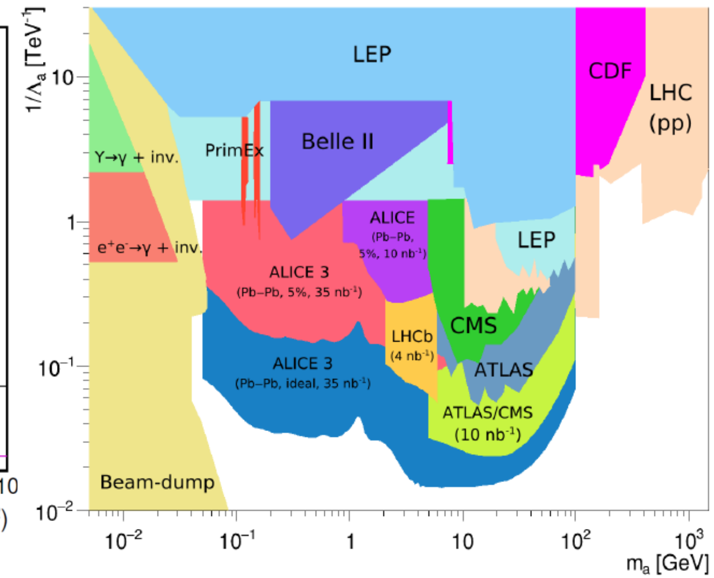

CERN Yellow Rep.Monogr. 7 (2019) 1159

Meson, channel	$\sigma^{Pb\text{-}Pb}$	N^{Tot}	$N^{\|\eta\| < 0.9}$	$N^{-4 < \eta < -2.5}$
$\rho^0 \to \pi^+ \pi^-$	5.2 b	68×10^9	5.5×10^9	-
$\rho' \to \pi^+ \pi^- \pi^+ \pi^-$	730 mb	9.5×10^9	210×10^6	-
$\phi \to K^+ K^-$	0.22 b	2.9×10^9	82×10^6	-
$J/\psi \to \mu^+ \mu^-$	1.0 mb	14×10^6	1.1×10^6	600×10^3
$\psi(2S) \to \mu^+ \mu^-$	30 μb	400×10^3	35×10^3	19×10^3
$\Upsilon(1S) \to \mu^+ \mu^-$	2.0 μb	26×10^3	2.8×10^3	880

$L^{Pb\text{-}Pb}$ = 13/nb

ALICE3 LOI: CERN-LHCC-2022-009 / LHCC-I-038

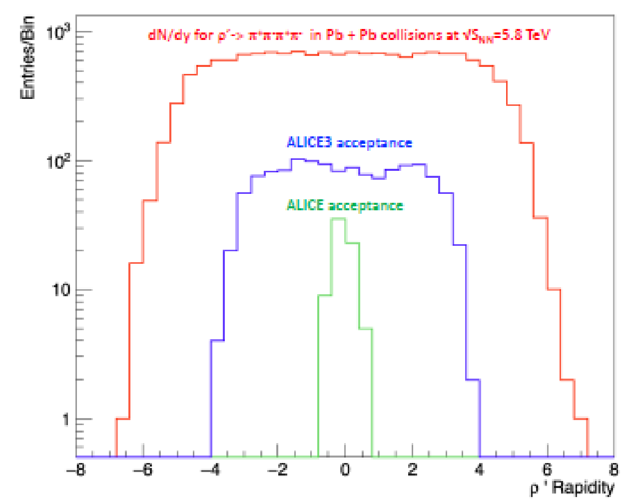

Summary

- Nuclear gluon structure probed with ρ^0, J/ψ and ψ(2S) at $x_B \sim 10^{-2} - 10^{-5}$
  - Measurements signal large nuclear gluon shadowing effects $S_{Pb} \sim 0.65$ at $x_B \sim 10^{-3}$ or $S_{Pb} \sim 0.5$ at $x_B \sim 10^{-5}$
  - No model currently describes the rapidity dependence
    - Models with shadowing or saturation describe data best at low x_B
    - Subnucleon fluctuations are important
- Proton gluon structure probed with J/ψ at $x_B \sim 10^{-2} - 10^{-5}$
  - No saturation visible at low $x_B \sim 10^{-5}$
  - More data needed (and more precise) to discriminate between models
- Photoproduction measured towards more central collisions
- Resonance-like structure found at dipion mass of 1.7 GeV
- We are limited by statistics and looking forward for Run 3 and beyond results

Backup

Comparison LHCb/ALICE – Pb-Pb @ 5 TeV

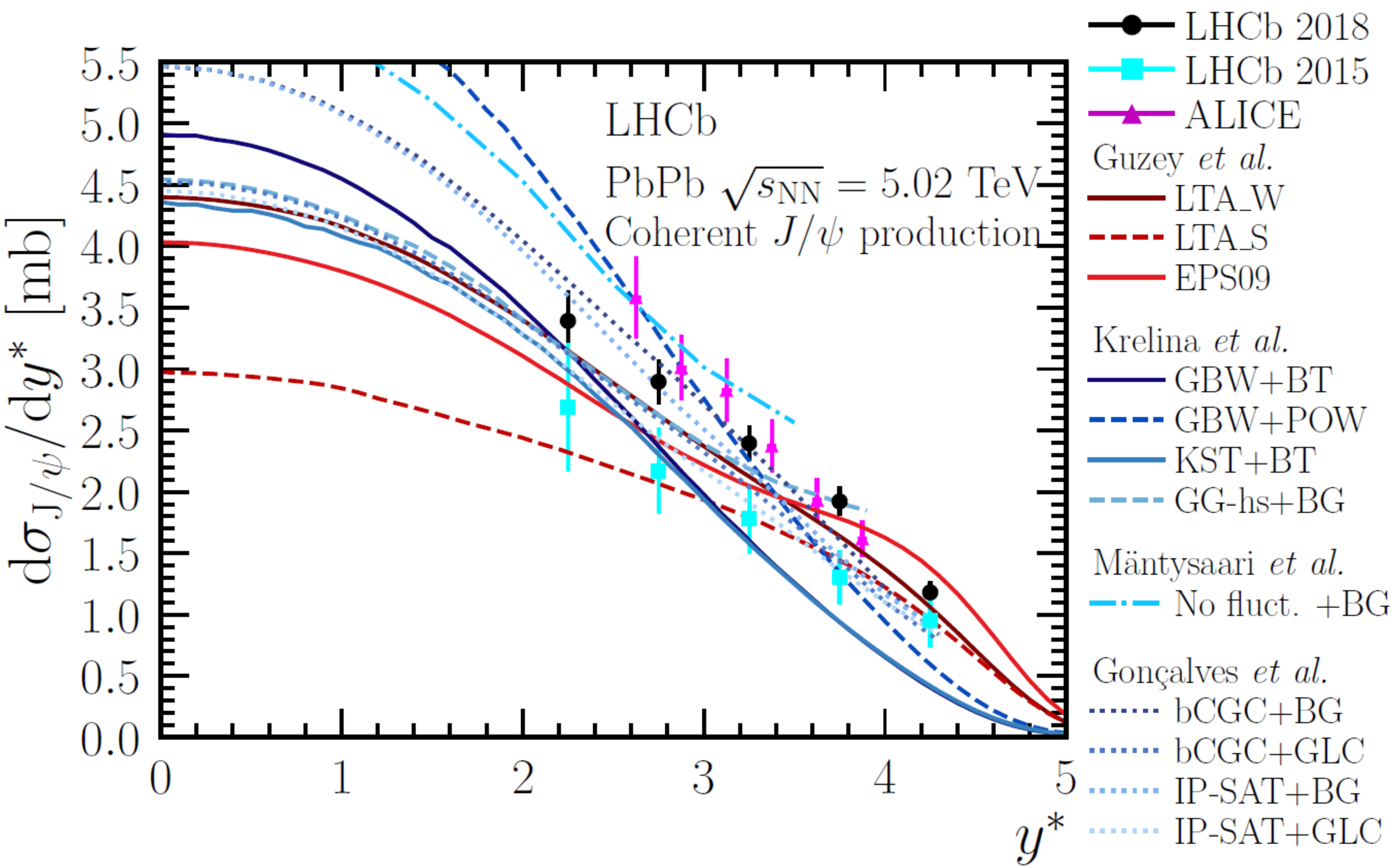

Articles

- ALICE
  - Coherent J/ψ photoproduction in ultra-peripheral Pb–Pb collisions at $\sqrt{s_{NN}}$ = 2.76 TeV, Phys. Lett. B718 (2013) 1273.
  - Charmonium and e + e − pair photoproduction at mid-rapidity in ultra-peripheral Pb–Pb collisions at $\sqrt{s_{NN}}$ = 2.76 TeV, Eur. Phys. J. C73, 2617 (2013).
  - Exclusive J/ψ photoproduction off protons in ultra-peripheral p-Pb collisions at $\sqrt{s_{NN}}$ = 5.02TeV, Phys. Rev. Lett. 113 (2014) 232504.
  - Coherent J/ψ photoproduction at forward rapidity in ultra-peripheral Pb-Pb collisions at $\sqrt{s_{NN}}$ = 5.02 TeV, Phys.Lett. B798 (2019) 134926.
  - Coherent J/ψ and ψ′ photoproduction at midrapidity in ultra-peripheral Pb-Pb collisions at $\sqrt{s_{NN}}$ = 5.02 TeV, Eur. Phys. J. C 81 (2021) 712.
  - First measurement of the |t|-dependence of coherent J/ψ photonuclear production, PLB 817 (2021) 136280.
  - Energy dependence of exclusive J/ψ photoproduction off protons in ultra-peripheral p-Pb collisions at $\sqrt{s_{NN}}$ = 5.02 TeV, Eur. Phys. J. C (2019) 79: 402.
  - Photoproduction of low-p_T J/ψ from peripheral to central Pb-Pb collisons at 5.02 TeV, arXiv:2204.10684 (2022).
  - Coherent photoproduction of ρ^0 vector mesons in ultra-peripheral Pb-Pb collisions at $\sqrt{s_{NN}}$ = 5.02 TeV, JHEP 06 (2020) 035.
  - First measurement of coherent ρ^0 photoproduction in ultra-peripheral Xe-Xe collisions at $\sqrt{s_{NN}}$ = 5.44 TeV, Phys. Lett. B 820 (2021) 136481.
- CMS
  - Coherent J/ψ photoproduction in ultra-peripheral PbPb collisions at $\sqrt{s_{NN}}$=2.76 TeV with the CMS experiment, Physics Letters B772 (2017) 489–511.
  - Measurement of exclusive ϒ photoproduction from protons in pPb collisions at $\sqrt{s_{NN}}$ = 5.02 TeV, Eur. Phys. J. C (2019) 79:277.
  - Measurement of exclusive $\rho(770)^0$ photoproduction in ultraperipheral pPb collisions at $\sqrt{s_{NN}}$ = 5.02 TeV, Eur. Phys. J. C 79, 702 (2019).
- LHCb
  - Updated measurements of exclusive J/ψ and ψ(2S) production cross-sections in pp collisions at $\sqrt{s}$ = 7 TeV, J. Phys. G 41 (2014) 055002.
  - Measurement of the exclusive ϒ production cross-section in pp collisions at $\sqrt{s}$ = 7 TeV and 8TeV, JHEP 09 (2015) 084.
  - Central exclusive production of J/ψ and ψ(2S) mesons in pp collisions at $\sqrt{s}$ = 13 TeV, JHEP 10 (2018) 167.
  - Study of coherent J/ψ production in lead-lead collisions at $\sqrt{s_{NN}}$ = 5TeV, arXiv:2107.03223v1 [hep-ex] (2021).
  - Study of the coherent charmonium production in ultra-peripheral lead-lead collisions, arXiv:2206.08221 [hep-ex] (2022).
  - J/ψ photo-production in Pb-Pb peripheral collisions at $\sqrt{s_{NN}}$ = 5TeV, Phys. Rev. C105 (2022) L032201.

VM cross section

$$\frac{d\sigma_{VM}^{coh}}{dy} = \frac{N_{VM}^{coh}}{\varepsilon_{VM} \times \varepsilon_{veto}^{pileup} \times \varepsilon_{veto}^{EMD} \times BR \times \mathscr{L}_{int} \times \Delta y}$$

$$N_{J/\psi}^{coh} = \frac{N_{yield}}{1 + f_I + f_D}$$

$$N_{\psi'}^{coh} = \frac{N_{yield}}{1 + f_I}.$$

- N_{yield} – J/ψ or ψ' raw yield,
- ε_{VM} - reconstruction efficiency
- f_I – incoherent contamination fraction
- f_D – feed down contamination fraction
- L_{int} – integrated luminosity
- Δy – rapidity interval
- BR – branching ratio of the Decay
- $\varepsilon^{pileup}_{veto}$ – pileup veto efficiency
- ε^{EMD}_{veto} – electromagnetic dissociation veto efficiency

Models

- **Black disk limit:**
  - Frankfurt, Strikman, Zhalov, *Phys. Lett.* B537 (2002) 51–61.
  - total cross section of the interaction is equal to $2\pi R_A^2$.
- **STARlight:**
  - Klein, Nystrand, Seger, Gorbunov, Butterworth, Comput. Phys. Commun. 212 (2017) 258–268; Klein and Nystrand, Phys. Rev. C 60 (1999) 014903.
  - Based on a phenomenological description of the exclusive production of VM off nucleons, the optical theorem, and a Glauber-like eikonal formalism, does not take into account the elastic part of the elementary VM–nucleon cross section.
  - Includes multiple scattering, **no gluon shadowing**.
- **GKZ (Guzey, Kryshen and Zhalov):**
  - Guzey, Kryshen, Zhalov, Phys. Rev. C93 (2016) 055206; Frankfurt, Guzey, Strikman, Zhalov, Phys. Lett. B752 (2016) 51–58.
  - Based on a modified **vector dominance model**, in which the hadronic fluctuations of the photon interact with the nucleons in the nucleus according to the Gribov-Glauber model of **nuclear shadowing**
- **GMMNS (Goncalves, Machado, Morerira, Navarra and dos Santos):**
  - Gonçalves, Machado, Moreira, Navarra, dos Santos, Phys. Rev. D96 (2017) 094027; Iancu, Itakura, Munier, Phys. Lett. B590 (2004) 199–208,
  - Based on the Iancu-Itakura-Munier (IIM) implementation of **gluon saturation** within the **colour dipole model** coupled to a boosted-Gaussian description of the wave function of the vector meson.
- **CCKT (Cepila, Contreras, Krelina and Tapia):**
  - Cepila, Contreras, Tapia Takaki, Phys. Lett. B766 (2017) 186–191; Cepila, Contreras, Krelina, Tapia Takaki, Nucl. Phys. B934 (2018) 330–340; N. Armesto, Eur. Phys. J. C26 (2002) 35–43
  - Based on the **colour dipole model** with the structure of the nucleon in the transverse plane described by so-called **hot spots**, regions of high gluonic density, whose number increases with increasing energy. The nuclear effects are implemented along the ideas of the Glauber model. Version without hot spots (named *nuclear*) and including them.
  - Indicates **gluon saturation**.

Models

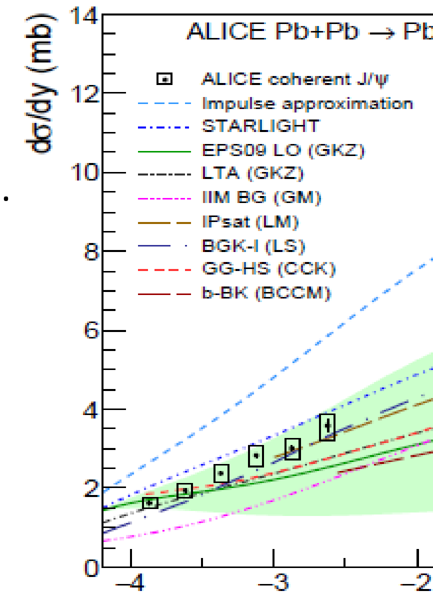

- **Impulse approximation:**
  - Exclusive photoproduction off protons, neglects all nuclear effects but coherence.
  - Based on STARlight.
- **EPS09 LO:**
  - GKZ model with parameterization of **nuclear shadowing** data.
  - Eskola, Paukkunen, Salgado, JHEP 04 (2009) 065.
- **LTA:**
  - GKZ model based on Leading Twist Approximation of **nuclear shadowing**.
  - Frankfurt, Guzey, Strikman, Phys. Rept. 512 (2012) 255–393.
- **IIM BG, IPsat, BGK-I:**
  - **Color dipole** approach coupled to the Color Glass Condensate (CGC) formalism with different assumptions on the dipole-proton scattering amplitudę.
  - **IIM BG:** Gonçalves, Moreira, Navarra, Phys. Rev. C 90 (2014) 015203; dos Santos, Machado, J. Phys. G 42 no. 10, (2015) 105001. (saturation)
  - **IPsat:** Lappi, Mäntysaari, Phys. Rev. C 83 (2011) 065202; Lappi, Mäntysaari, Phys. Rev. C 87 (2013) 032201. (saturation)
  - **BGK-I:** A. Łuszczak, Schäfer, Phys. Rev. C 99 no. 4, (2019) 044905. (shadowing)
- **GG-HS**:
  - CCK **color dipol model** with **hot spots** nucleon structure with Glauber-Gribov formalism
  - Cepila, Contreras, Krelina, Phys. Rev. C 97 no. 2, (2018) 024901; Cepila, Contreras, Tapia Takaki, Phys. Lett. B766 (2017) 186–191.
- **b-BK:**
  - Bendova, Cepila, Contreras, Matas (BCCM) model based on the **color dipole** approach coupled to the impact-parameter dependent Balitsky-Kovchegov equation with initial conditions based on the Woods-Saxon shape of the Pb nucleus.
  - Bendova, Cepila, Contreras, Matas, Physics Letters B 817 (2021) 136306.